



AUTHOR:

TITLE:

YEAR:

OpenAIR citation:

This work was submitted to- and approved by Robert Gordon University in partial fulfilment of the following degree:

OpenAIR takedown statement:

Section 6 of the “Repository policy for OpenAIR @ RGU” (available from <http://www.rgu.ac.uk/staff-and-current-students/library/library-policies/repository-policies>) provides guidance on the criteria under which RGU will consider withdrawing material from OpenAIR. If you believe that this item is subject to any of these criteria, or for any other reason should not be held on OpenAIR, then please contact openair-help@rgu.ac.uk with the details of the item and the nature of your complaint.

This is distributed under a CC _____ license.

Role of Nuclear Factor Kappa B (NF κ B) in the vascular complications of diabetes

Fatima Mohamed Al Ali

A thesis submitted in partial fulfilment of the requirements of the
Robert Gordon University
for the degree of Master of Research (MRes)

School of Pharmacy and Life Sciences,
Robert Gordon University
Aberdeen

2016

Abstract

Role of Nuclear Factor Kappa B (NFκB) in the vascular complications of diabetes

Fatima Mohamed Al Ali

for the degree of Master of Research (MRes)

Diabetes mellitus (DM) is the most common metabolic disease worldwide. This condition accounts for the majority of renal failure and blindness in adult's aged between 20 to 74 years of age. After 20 years, some of type 1 diabetic patients and around 60% of type 2 diabetic patients will be diagnosed with retinopathy. In 2011, a survey was presented and supplied data on the number of people who are suffering from diabetes. In Scotland, they found that 247,278 people were diagnosed with diabetes. In addition, about 36.6% of patients' were diagnosed with type 1 diabetes (T1DM) and 31.7% of those with type 2 diabetes (T2DM).

In this research, the role of inflammatory mediators in the progression of the vascular complications of diabetes was investigated. Specifically, the role of nuclear factor kappa B1 (NFκB1). There were 2 approaches used in this study: i) a bioinformatics approach to determine what single nucleotide polymorphisms (SNP) may occur within the NFκB1 gene in T2DM and ii) a molecular biology approach to investigate the role of the SNP of interest in a human monocyte cell line using polymerase chain reaction (PCR) and restriction enzymes.

Methods

Genetic polymorphisms were investigated using bioinformatics tools through computational analysis and databases, such as, Ensembl and the National Center for Biotechnology Information (NCBI), NEB cutter, Primer Quest and NetPhos. The SNP of interest was identified due to its role in diabetes. Primers were designed to span the region for the SNP of interest, amplified using PCR and resolved in an agarose gel. The SNP of interest was restricted with three restriction enzymes (HpyCH4iii, Alu1 and PvuII) followed by sequencing of the product. The U937 monocyte cell line was used to investigate the expression of the NFκB gene. Cells were incubated in RPMI 1640 with 2 mM L-glutamine, 100 U/mL Penicillin, Streptomycin and 10% heat inactivated foetal bovine serum (FBS) with H₂O₂ for up to 180 minutes with 5.5mM, 20mM and 40mM glucose +/- H₂O₂. RNA extraction was followed by cDNA amplification, which was subsequently used in reverse transcriptase polymerase chain reaction (RT-PCR) and for a period of time to address the biological significance of NFκB activation in these conditions.

Results

A DNA fragment corresponding to the 206bp fragment was identified that spanned the area containing the SNP. Successful restriction with HpyCH4iii has not been possible, therefore, DNA sequencing was

carried out. Sequencing identified the A allele indicating the presence of the homozygous wild type form of this region.

Also, determining the role of NF κ B activation, HIF1- α and β 2-microglobulin in U937 cells mRNA via culturing U937 under high glucose (HG) condition in different concentrations (5.5mM, 20mM and 40mM). The NF κ B and β 2-microglobulin PCR product was not detected during incubations with various glucose concentrations.

Conclusion

The DNA sequence of the U937 cell line corresponds to the wild type form of the SNP under investigation. This model has enabled the investigation of the effect of glucose concentration on the expression of the NF κ B and HIF1 α genes and this has provided useful insight that can be used to develop this work further.

Keywords: diabetes, type 1 diabetes, type 2 diabetes mellitus, diabetes retinopathy, pathogenesis of diabetes, nuclear factor kappa B (NF κ B), bioinformatics, U937 cell line, SNP detection, rs230539.

Acknowledgments

First of all, praise be to Allah, who blessed me with the ability to accomplish this work, for his kindness and great generosity.

I would like to thank my principal supervisor, Dr. Rachel Knott for her encouragement, patience and her guidance, comments and for help me whenever I was in need. In other words, her good leading.

I would to thank Dr.Gemma Barron my co-supervisor for her encouragement and for helping me with the lab work.

Thanks to Institute of Health and Wellbeing and Administrative department staff, especially Mrs. Andrea MacMillan. In addition, I would like to thank all technical staff especially Mr. Chris Fletcher, who try to help me whenever I need. I also would like to thank Dorothy McDonald and Martin Simpson for the administrative help on the research.

I am highly indebted to my family especially my husband for supporting me and giving me the strength to continue my education.

I would also like to thank Sidra Medical Research Center for awarding me scholarships throughout my study.

Thank you all.

Abbreviations

AGEs	Advanced glycation end products
AR	Aldose reductase
BAFFR	B-cell-activating factor receptor
cDNA	Complementary Deoxyribonucleic acid (DNA)
DAG	Diacylglycerol
DHAP	Dihydroxyacetone phosphate
DI	Diabetes insipidus
DM	Diabetes mellitus
DNA	Deoxyribonucleic acid
DR	Diabetic retinopathy
gDNA	Genomic DNA
GFAT	Glutamine fructose-6-phosphate amidotransferase
ICAM	Intracellular adhesion molecule
IDDM	Insulin dependent diabetes mellitus
IL	Interleukin
INOS	Inducible nitric oxide synthase
LTbR	Lymphotoxin beta receptor
mRNA	Messenger Ribonucleic acid
NADPH	Nicotinamide adenine dinucleotide phosphate
NCBI	National Center for Biotechnology Information
NFκB	Nuclear factor kappa B
NIDDM	Non-insulin dependent diabetes mellitus

NO	Nitric oxide
NPDR	Non-proliferative diabetes retinopathy
RAGE	Receptor for AGEs
PCR	Polymerase chain reaction
PDR	Proliferative diabetes retinopathy
PKC	Protein kinase C
RNA	Ribonucleic acid
ROS	Reactive oxygen species
SNP	Single nucleotide polymorphism
TBARS	Thiobarbituric acid-reactive substances
T1DM	Type 1 diabetes mellitus
T2DM	Type 2 diabetes mellitus
TNF α	Tumour necrosis factor-alpha
UDP	Uridine diphosphate
UDP-GlcNAc	(UDP)-N-acetylglucosamine
UTR	Untranslated region
VCAM-1	Vascular cell adhesion molecule-1
VEGF	Vascular endothelial growth factor
VEGFR	Vascular endothelial growth factor receptor

Table of Contents

List of Figures	9
List of Tables	10
Chapter 1: Introduction.....	11
1.1 Diabetes.....	12
1.2 Diabetic retinopathy.....	14
1.3. Diabetic retinopathy and the immune response.....	17
1.3.1.1 Polyol pathway flux.....	20
1.3.1.2 Protein kinase C.....	22
1.3.1.3 Advanced glycation end products.....	25
1.3.1.4. Oxidative stress.....	25
1.3.1.5 Hexosamine pathway activation.....	26
1.4 Nuclear factor kappa B.....	29
1.4.1 The relationship between NFκB and diabetes.....	29
1.5 Rationale for study.....	35
Chapter 2: Materials and Methods.....	36
2.1. <i>Materials</i>	37
2.2. <i>Methods</i>	38
2.2.1 Bioinformatics.....	38
2.2.2 Cell culture and cell counting.....	40
2.2.3 DNA extraction and purification.....	42
2.2.4 Polymerase chain reaction (PCR).....	43
2.2.5 Gel electrophoresis.....	44
2.2.6 Restriction digest.....	45
2.2.7 PCR purification.....	47
2.2.8 Sequencing.....	48
2.3 RNA extraction and purification.....	48
2.3.1 RNA extraction using RNeasy mini kit.....	48
2.3.2 RNA extraction using TRIzol reagent.....	50

2.4 cDNA synthesis and reverse transcriptase polymerase chain reaction (RT-PCR)	51
Chapter 3.Results	54
3.1 Bioinformatics output.....	55
3.1.1 Detection of SNPs and identification of the NFκB1 region	55
3.1.2 Impact of SNPs.....	60
3.1.2.1 Identification of the phosphorylation site	60
3.1.2.2 Primer design for PCR.....	63
3.1.3 DNA detection.....	64
3.1.4 DNA Sequencing	68
3.1.4.1 PCR purification and DNA detection.....	68
3.1.4.2 Sequence output.....	69
3.2 RNA Detection.....	71
3.2.2 cDNA amplification with HIF1α and NFκB.....	75
3.2.3 cDNA amplification with NFκB and HIF1 α (Control (C) and H ₂ O ₂).....	77
3.2.4. cDNA amplification with NFκB, HIF1 α and β2-microglobulin with different glucose concentrations	79
<i>Chapter 4: Discussion</i>	82
4.1 SNP detection	83
4.2 Standardisation of NFκB, RT-PCR and the effect of different glucose concentrations.....	84
4.3 Conclusion.....	87
4.4 Future Work.....	87
<i>References</i>	89

List of Figures

Figure 1: Polyol Pathway	21
Figure 2: PKC Pathway.....	23
Figure 3: Hexosamine Pathway	28
Figure 4: Human NFκB1 Structure	29
Figure 5: Classical and Alternative Pathways of NFκB.....	33
Figure 6:Restriction Enzymes.....	45
Figure 7: Chromosome 4.....	56
Figure 8: Sequence of interest, identified phosphorylation sites and predicted score.....	61
Figure 9: rs230539 Sequence.	64
Figure 10:PCR product following amplification with NFκB primers	65
Figure 11: A1 hr incubation with HpyCH4iii at 37°C	66
Figure 12: Restriction with HpyCH4iii, Alu1 and PvuII	67
Figure 13: PCR purification	68
Figure 14: (A) Predicted DNA sequence and (B) DNA sequence obtained from Dundee.....	69
Figure 15: Sequence Alignment.....	70
Figure 16: Restriction sites for enzymes HpyCH4iii and Alu1	71
Figure 17: RNA gel electrophoresis of RNA bands	72
Figure 18: Gel electrophoresis for cDNA amplification with β-Actin.....	73
Figure 19: Gel electrophoresis for cDNA amplification with β-Actin.....	74
Figure 20: Gel electrophoresis for PCR samples with HIF 1α.....	75
Figure 21:Gel electrophoresis cDNA amplification with NFκB.....	76
Figure 22:Gel electrophoresis cDNA amplification with NFκB and HIF1α.....	77
Figure 23: Gel electrophoresis for cDNA amplification with HIF1 α	78
Figure 24: Gel electrophoresis for cDNA amplification with 0.2 μM NFκB and HIF1α in different glucose concentrations	79
Figure 25: Gel electrophoresis for cDNA amplification with 0.2 μM HIF1α and β2-microglobulin α in different glucose concentrations.....	80

List of Tables

Table 1: Bioinformatics websites used for in silico analysis	38
Table 2: NFκB Forward and Reverse Primers used in PCR.	44
Table 3: Samples prepared for digestion	47
Table 4: RNA concentration for 1×10^7 U937 cells	50
Table 5: Details of primers used for PCR.	53
Table 6: Summary of NFκB1 variants (SNPs) identified in NFκB	58
Table 7: Variations of NFκB1 in Humans associated with disease.....	59
Table 8: Details of variant rs230539.....	59
Table 9: Score and Qualitative Prediction	63

Chapter 1: Introduction

This thesis shall present work relating to the role of nuclear factor kappa B1 in the vascular complications of diabetes. This work has been carried out through investigation of genetic polymorphisms within the NFκB1 gene using *in silico* analysis and investigation of the regulation of NFκB1 mRNA in a human monocyte U937 cell line. This chapter begins with an overview of diabetes in terms of causes, types and the role of mechanistic pathways. Secondly, an overview of nuclear factor kappa B and the relationship between NFκB and diabetes will be presented followed by a description of the rationale for this study.

1.1 Diabetes

Diabetes mellitus (DM) and diabetes insipidus (DI) are both chronic medical conditions. DM is caused by insulin deficiency and/or insulin resistance, whereas, DI is an insufficiency of vasopressin secreted through the pituitary gland (Di Iorgi *et al.* 2012). Diabetes mellitus is classified into two forms: Type 1 and Type 2 (Allman 2008).

1.1.1 Type 1 diabetes mellitus

Type 1 diabetes mellitus (T1DM), also known as insulin-dependent diabetes, is characterised by damage to the pancreatic β-cells, which is often caused by autoimmune processes such as autoantibodies to insulin (Faideau *et al.* 2005). Within the pancreatic islets of Langerhans, autoantibodies bind to β cells, which in turn stimulate T cells leading to the autoimmune destruction of these cells and thus the loss of insulin production which results in T1DM (Faideau *et al.* 2005). Insulin is released from the pancreas into the bloodstream, and is responsible for, not only, controlling how the body utilises carbohydrate and fat found in food, but also for the regulation of the metabolism of glucose absorbed into the bloodstream from food. T1DM

is characterised by insulinitis, which may result in islet cell inflammation and also in β -cell damage. During T1DM, the inflammatory lesion occurs inside islets and these were identified by the absence of insulin production and cause an increase in the number of cells that are responsible for the immune response including T-lymphocytes, B lymphocytes and macrophages (Atkinson 2012).

1.1.2 Type 2 diabetes mellitus

Type 2 diabetes mellitus (T2DM), previously known as adult onset or non-insulin-dependent diabetes, is diagnosed when an inadequate amount of insulin is released and/or the insulin being released is ineffective in target tissues such as muscle and liver cells (Williamson 2009), precipitating a condition known as insulin resistance (Aiello 2002; Alghadyan 2011). This results in high levels of circulating glucose. The incidence of T2DM is known to increase with age, adiposity and genetic factors and, there are also lifestyle aspects, such as, obesity that can contribute to the onset and the progression of this condition (Ma & Chan 2013).

1.1.3. Diabetes insipidus

Diabetes insipidus (DI) is a kidney disorder which is in contrast to T1DM. In DI, high blood sugar is not present and immoderate urination, which is caused by inadequate supplies of the anti-diuretic hormone (ADH) that known as vasopressin, can lead to an increased salt concentration (Di Iorgi *et al.* 2012). It is a kidney disorder that is caused by insufficient vasopressin released by the pituitary gland (Serono 2011).

1.1.4 Vascular complications of diabetes mellitus

T1DM and T2DM are health conditions associated with blood glucose concentrations that are raised to a level that adversely influences the body's physiology and the function of a variety of organs, including the kidneys, eyes and heart (Allman 2008).

There are two main types of complications associated with DM, namely macrovascular and microvascular complications. Macrovascular complications affect large vessels such as cardiac and cerebrovascular vessels, triggering the process of atherosclerosis, which leads to the narrowing of arterial walls throughout the body (Fowler 2008).

Microvascular complications, according to Chistiakov (2013), affect the small vessels in the eyes, kidneys and other vital organs of the body, leading to a multiplicity of complications including diabetic retinopathy, neuropathy and nephropathy. Prolonged hyperglycemia is a major cause of vascular complications that are associated with diabetes (Cade 2008). Hyperglycemia activates oxidative stress, which has a role in enhancing vascular complications. Extant literature demonstrates that the most common microvascular complication is diabetic retinopathy (Sivaprasad *et al.* 2012) and this particular vascular complication will be the focus of this thesis.

1.2 Diabetic retinopathy

Diabetic retinopathy (DR) is the leading cause of blindness among the adult population (Chistiakov 2011). A common complication in T1DM patients after diagnosis is DR; and current statistics demonstrate that over 60% of individuals presenting with T2DM will also suffer from DR (Saxena 2012). Furthermore, a recent study conducted in the United Kingdom shows that 60% of patients with type 2 diabetes are affected by retinopathy (Diabetes UK 2010).

DR is sub-classified into two stages: an early non-proliferative stage and a later proliferative stage. During the early stages, pericyte deficient capillaries and saccular capillary microaneurysms are identified. As posited by Saxena (2012), mechanisms for retinal capillary retrogression include the blockage by white blood cells or platelets of the vessel lumen, leading to endothelial cell death and capillary destruction. In DR, high concentrations of glucose accumulate inside blood vessels of the retina and in other tissues leading to a complex series of changes to biochemical pathways leading to functional changes (Kerry 2013).

The most common characteristics of non-proliferative DR include haemorrhages, microaneurysms, microinfarcts and the production of exudates. The first sign of retinopathy is a microaneurysm, which manifests as an enlargement of the capillary wall and appears as small red dots on the retina (Alghadyan 2011). Small caliber retinal vessels, such as arterioles and capillaries, are the main casualties in diabetic retinopathy, with research showing that the damage causes microvascular occlusion, which in turn leads to hypoxia and the development of new vessels (Saxena, 2012). Macular oedema, according to this particular author (Saxena, 2012), also results from microvascular leakage. Blood vessels consist of two types of interacting cells. One of these cells is endothelial cells, which form the inner lining of the vessel wall and the other cell type is the pericyte (Saxena, 2012).

Pericytes are a specialised type of vascular smooth muscle cell that can be found in close association with blood capillaries. The normal retina has a high pericyte density. Diabetic patients are likely to develop DR and this loss of pericytes cells is an early feature of diabetic retinopathy. The reason for pericyte damage is thought to be hyperglycemia when damage leads to serious effects, which cause microaneurysms and weakness of the vascular walls (Bergers & Song 2005).

The presence of abnormal retinal vessels triggers the leakage of proteins and lipoproteins, not to mention the bursting of weak

capillaries often causes haemorrhages that appear in the deep layer of the retina (Alghadyan 2011). The progression of new vessels on the optic disk also occurs in proliferative diabetic retinopathy (PDR). Neovascularization and preretinal haemorrhage are the first signs of early PDR, with neovascular glaucoma following in late phases of disease progression (Alghadyan 2011).

Animal studies show that pericytes vanish before endothelial cells are lost and acellular capillaries with no blood supply remain (Hammes *et al.* 2011). Thus even before endothelial damage is evident the vessel function is compromised. The leakage of retinal capillaries and the associated ischemic retina increases the potential for an angiogenic response from the surrounding areas of capillaries leading to PDR (Hammes *et al.* 2011).

Monocyte accumulation may also participate in the progression of DR and can lead to neovascularization and a detached retina (Marumo *et al.* 1999). There is an important growth factor known as vascular endothelial growth factor (VEGF) that is associated with DR and has a vital role in progression of diabetic complications (Marumo *et al.* 1999). In addition, hyperglycemia causes a rise in VEGF expression in aortic smooth muscle cells (Duh & Aiello 1998). VEGF is a moderator of vascular permeability and angiogenesis in the pathogenesis of DR (Andreasen *et al.* 2011).

VEGF is one of the main growth factors that act during angiogenesis, which is central for the creation of new blood vessels (Roy 2006). Angiogenesis is activated by VEGF in several pathological conditions such as tumor growth, wound healing, cardiovascular disease, embryogenesis and ocular neovascularisation. An increased level of VEGF-A expression has been the consequence in DR in humans (Roy 2006) with elevated levels of VEGF-A resulting in vascular leakage and neovascularization in DR (Roy 2006). The failure of the vascular wall in diabetes is the consequence of chronic hyperglycemia. Therefore, chronic hyperglycemia is a key factor for vascular dysfunction. Advanced glycation end products pathway (AGEs) result from increased blood glucose levels. Increased accumulation of AGEs takes place in the

vasculature. AGEs influence blood vessels by different receptor pathways such as macrophage scavenger receptor (MSR) type II, galectin-3, CD36 and receptor for AGEs (RAGE). For instance, interaction between AGE and RAGE (AGE-RAGE) activates the expression of pro-inflammatory molecules and NFκB. In addition, AGE and RAGE interact with several ligands such as amyloid-β peptide, macrophage-1 antigen (MAC-1) and this interaction causes the activation of the mitogen-activated protein kinase (MAPK p38) pathway. Expression of these molecules contribute to the progression of vascular complications (Roy 2006).

Large vessels are composed of vascular smooth muscle cells (VSMCs), endothelium and adventitia. VSMC has an important role in controlling of blood pressure, for that reason, VSMC layers decrease with vessel size and are not present in the capillary. The high numbers of pericytes are important when considering endothelial proliferation, regulation and angiogenesis and have a role in the support of the endothelium (Andreasen *et al.* 2011).

The risk of DR may be controlled to an extent with good diabetes management and the sight-threatening disease may be treated by laser photocoagulation and vitrectomy (Tarr *et al.* 2013) but, clearly an alternative approach is needed.

1.3. Diabetic retinopathy and the immune response

Several intriguing findings from studies containing patient samples and animal models show that DR is associated with chronic inflammation: including cytokines and chemokines, which in turn activate leukocytes and endothelium (King 2008). In addition, according to King (2008), there are diverse inflammatory shifts associated with DR, including increased cytokine levels and adhesion molecules, as well as mounting vasocclusion. Evidence indicates that leukocytes can block capillaries

and this is a result of the huge size of these cells in relation to the size of the capillaries and the stiffness of the cytoplasm (Schröder *et al.* 1991). Endothelial cells enlarge and the capillary tightens in conditions of low perfusion pressure and during the early stages of diabetes (Schröder *et al.* 1991). The release of chemotactic factors and expression of adhesion molecules on endothelial cells can lead to increasing adhesive stress between the endothelium and leukocytes. The stimulation of monocytes is associated with the production and release of oxygen free radicals and proteases. This activation leads to microvascular injury (Schröder *et al.* 1991). Indeed, some experiments show that tumor necrosis factor alpha (TNF- α) and interleukin-1 beta (IL-1 β) are elevated in the serum of patients suffering from DR (Nehme & Edelman 2008). Consequently, the stimulation of these cytokines is inarguably associated with the pathogenesis of DR, which in effect is stimulated by an increase of glucose level in human monocytes (Nehme & Edelman 2008). An animal study (in diabetic rats) (Schröder *et al.* 1991) shows that monocytes cluster within the DR lesion, which indicates that monocyte recruitment is increased through disease progression. Hyperglycemia has been reported to encourage expression of inflammatory molecules such as IL-6, IL-8, vascular cell adhesion molecule 1 (VCAM-1) and monocyte chemoattractant protein 1 (MCP-1). Also, there are endothelial alterations caused by hyperglycemia such as increasing adhesion molecule expression that enhance platelets and monocyte adhesion to the endothelium. Increased activity of endothelial cells causes monocytes to move into the vascular tissue, which transform to a macrophage. The macrophages act as a local source of pro-inflammatory molecules (Andreasen *et al.* 2011).

Immunity within the retina is critical during infections and inflammation. There is a special cell in the retina known as the retinal pigment epithelium (RPE), which in turn has an important role in immune defense. The RPE is composed of one layer of neural cells, which are located among the neural retinal photoreceptors and choroid cell (Detrick *et al.* 2010). There are several functions for the RPE cells including nutrient transportation from the choroid to the retina and transfer of waste in the opposite direction. The role of this cell is as an

antigen presenting cell (APC) that regulates both innate and adaptive immune responses. Therefore, they express Toll-Like receptors (TLRs), complement components, Fc-gamma receptors and major histocompatibility complex (MHC) class I and II molecules. This leads to the production of cytokines, chemokines, and growth factors and proinflammatory molecules including, IL-6, IL-8, MCP-1, and sICAM-1. IFN- β is highly expressed by the RPE cell (Detrick *et al.* 2010).

There are some studies that show that TGF- β stimulates RPE cells to produce VEGF and can inhibit T-cell function (Detrick *et al.* 2010). Moreover, the RPE cell produces suppressive molecules including TGF- β , IL-11, and IFN- β cell (Detrick *et al.* 2010). In addition, the basic site for retinal changes and damage is the RPE cell, which has significant effects in optical diseases such as DR (Detrick *et al.* 2010).

NF κ B located in microvessels of the retina and its stimulation is in charge of pericyte damage in DR (Song *et al.* 2012). The activity of NF κ B is operated through phosphorylation, which induced degradation of regulatory proteins, which are known as NF κ B inhibitors (I κ B) (Sandip 2009). There are several members of I κ B family: I κ B α , I κ B β , I κ B γ and Bcl-3. These members have 33 amino acid sequences known as ankyrin repeats, which intermediately attach to NF κ B dimers and increase the activity of NF κ B (Sandip 2009).

NF κ B is activated when I κ B is degraded. Through this stimulation, I κ B α is phosphorylated on serine residues by I κ B kinase. Phosphorylation leads to the production of I κ B α , which is a substrate for ubiquitination on lysine residues. This molecule causes degradation of the protein by the 26S proteasome (Donnelly, *et al.* 2004).

1.3.1 Pathogenesis of diabetic retinopathy

There is a study that shows that most of T1DM patients and >60% of T2DM patients can suffer from DR (Tarr *et al.* 2013). Several factors, including age, control of glycaemia, pregnancy, control of blood pressure, renal failure and hyperlipidemia (abnormally elevated levels

of any or all lipids and/or lipoproteins in the blood stream), are known to contribute to the initiation and progression of DR. Moreover, biochemical shifts play a considerable role in the occurrence of hyperglycemia (Alghadyan 2011). Alghadyan (2011) acknowledges the existence of several biochemical changes, including increased polyol pathway flux, activation of protein kinase C (PKC), elevation of oxidative stress, formation of AGEs and activation of hexosamine pathway. These important pathways are briefly described below as they relate to DR and are the subject of a hypothesis suggested by Michael Brownlee (Brownlee 2005).

1.3.1.1 Polyol pathway flux

This is a metabolic pathway where glucose is converted into sorbitol by the enzyme aldose reductase (AR), using as a co-factor nicotinamide adenine dinucleotide phosphate (NADPH) (as shown in Fig 1). Sorbitol dehydrogenase oxidises sorbitol to fructose and nicotinamide adenine dinucleotide (NAD⁺) (Aveleira 2009). Researchers have found that AR is involved in diabetes, particularly in reference to the observation that in hyperglycemia, AR begins to convert glucose to sorbitol using the co-factor NADPH (Aveleira 2009). Animal studies in diabetic rats demonstrate that the AR is present in the retina when the glucose concentration is high and has a significant role to play in DR pathogenesis (Balasubramanyam *et al* 2002). Osmotic damage mediated by sorbitol leads to retinal capillary basement membrane thickening and the use of aldose reductase inhibitors (ARIs) can reduce the thickness of this membrane (Balasubramanyam *et al* 2002). One example of ARI is Sorbinil, which can minimize the swelling of small blood vessels in retina (Balasubramanyam *et al* 2002). There is a drug not tested in humans called ARI-809, which was used to prevent retinopathy in animals and it worked successfully (Ahmad 2013).

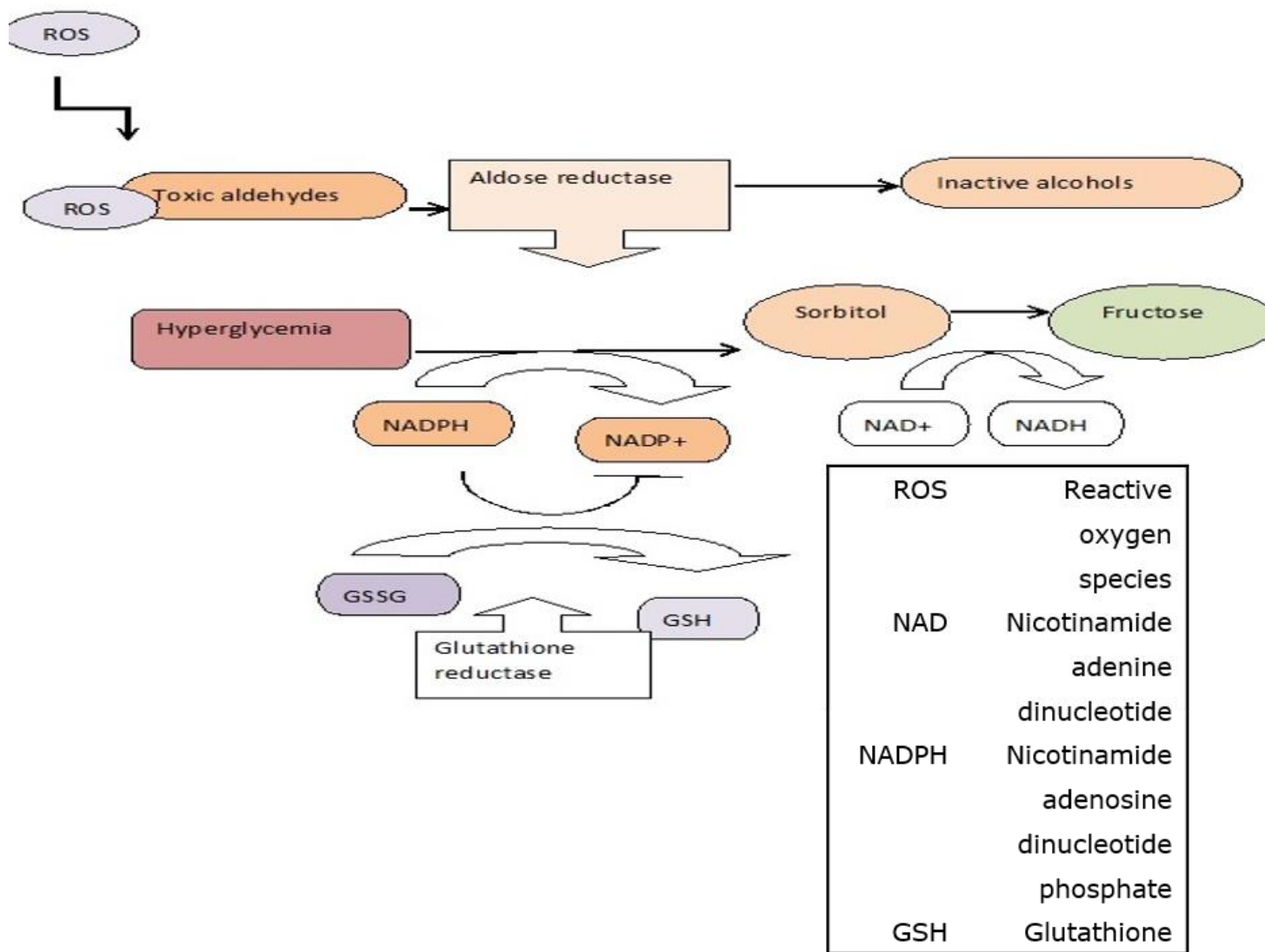


Figure 1: Polyol Pathway, this pathway induced oxidative stress during hyperglycemia. Sorbitol accumulates and produces osmotic stress, Adapted from Brownlee (2001)

1.3.1.2 Protein kinase C

Protein kinase C (PKC) is another important biochemical-signalling pathway, whereby the activity of PKC increases in response to hyperglycemia. There are several cellular changes arising from PKC activation, with the most important being the increased permeability of the retinal vasculature and changes in blood flow to the retina (Alghadyan 2011). Another shift is neovascularisation, which arises when the basement membrane thickens causing ischemia, which in turn activates hypoxia inducible factor type 1 (HIF-1) (Alghadyan 2011). HIF-1 increases the expression of VEGF (Alghadyan 2011). PKC is also involved in the stimulation of the expression of the VEGF gene which is also activated by HIF1 (Semeza *et al* 1998). The stimulation of PKC results when hyperglycemia enhances the production of diacylglycerol (DAG), which in turn stimulates PKC classic isoforms (α , β and δ) cofactors (as shown in Fig 2).

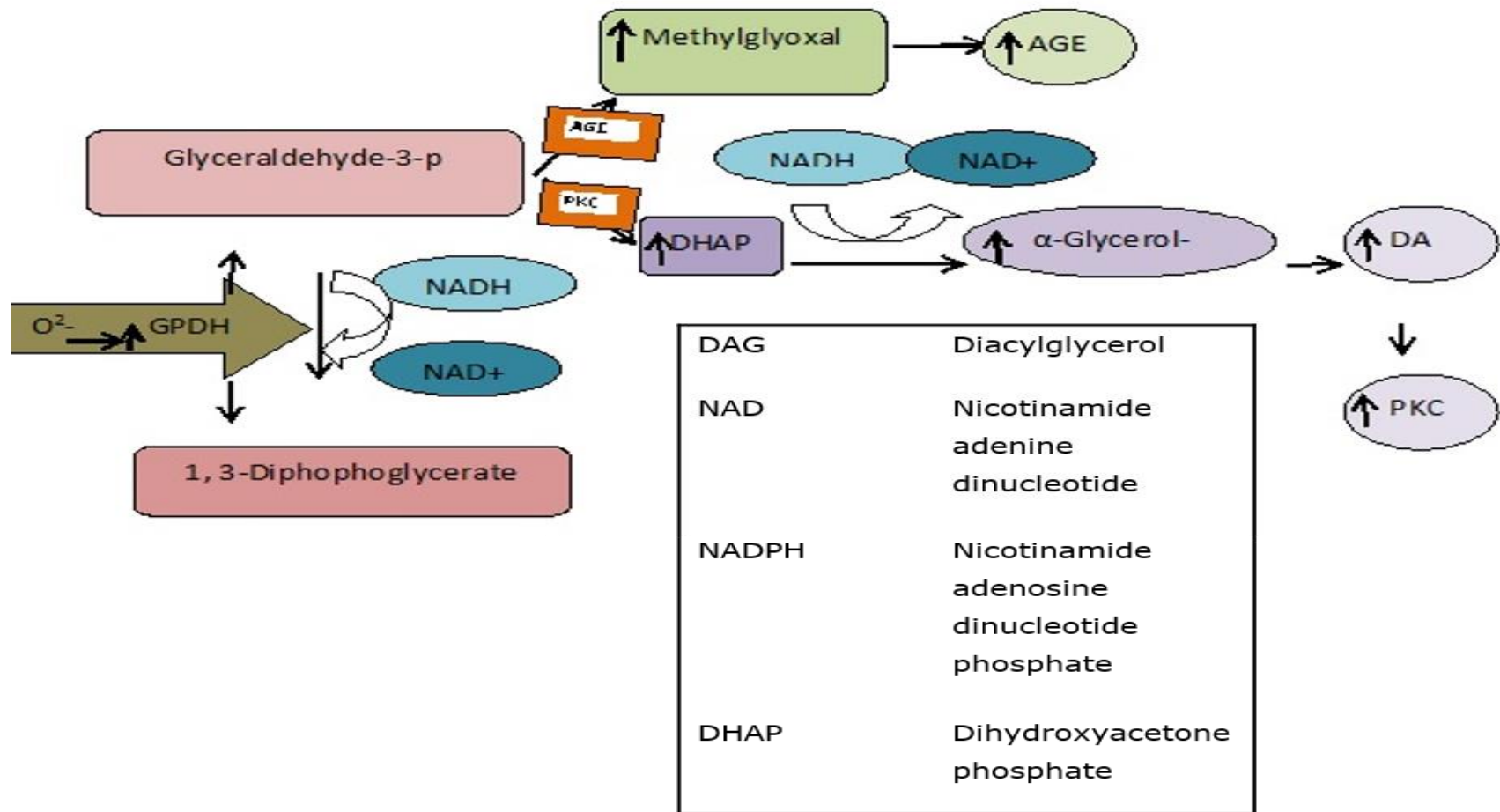


Figure 2: PKC Pathway, hyperglycemia induced PKC activity when the glucose metabolised to glycolytic intermediates *via* enhances the production of diacylglycerol (DAG), Adapted from Alghadyan (2011). Also, hyperglycemia increases advanced glycated end-products (AGEs), which in turn activates AGE receptors and cause the activation of DAG and PKC (Sandip 2009)

PKC isoforms are divided into three groups; these groups are the classic group (cPKCs), the novel group (nPKCs) and the atypical group (aPKCs). The classic group includes cPKC- α , β I, β II, and γ and activation of this group needs phospholipid and calcium. The novel group includes nPKC- δ , ϵ , η , θ , and μ and activation of this group requires phospholipid only. The atypical group includes aPKC- ι , ζ , and ξ and there is no requirement for calcium or phospholipid for activation (Donnelly *et al* 2004). PKC exists as a family of 15 isoforms (Fhearraigh) which acts as an important connection to the progression of DR (Lang 2007). Regulation of PKC isoforms occurs by generating DAG *via* activation and production of phosphoinositides and phosphatidic acid. In the case of hyperglycemia, DAG is generated via glyceraldehyde-3-phosphate (G3P), dihydroxyacetone phosphate (DHAP) and alpha-glycerol-phosphate (Lebovitz 2001). Lebovitz (2001) acknowledges that PKC phosphorylates serine and/or threonine kinase and this alters the intracellular function of a number of different proteins. The stimulation of PKC mediates neovascularisation and is vital in VEGF signalling, which has an important function in the initiation and progression of diabetes and DR (Lang 2007). While it has been demonstrated that high glucose concentration stimulates PKC via the Polyol pathway and reactive oxygen species (ROS) production, hyperglycaemia stimulates PKC- β , which is evident in tissues such as the retina. This activation is responsible for causing several changes such as the increased vascular permeability. Consequently, there exists compelling evidence to suggest that the PKC pathway is important in hyperglycaemia and DR because it stimulates NF κ B, which in turn enhances the expression of pro-inflammatory genes (Brownlee 2005).

1.3.1.3 Advanced glycation end products

Prolonged hyperglycemia can cause the formation of advanced glycated end-products (AGEs) when hyperglycaemia stimulates non-enzymatic glycation of proteins. AGEs work *via* cell receptors, which lead to oxidative stress and cause further diabetic complications (Sandip 2009). AGE products are formed by one of two pathways that impact upon vascular effects, namely receptor-independent and receptor-dependent pathways. Oxidative stress and NFκB activation result from interaction of AGEs with their receptors (AGE-R1, AGE-R2 and AGE-R3). Extant literature demonstrates that vascular endothelial damage; microaneurysm formation and dysfunction of vasculature are related to aggregation of AGEs in the retina of diabetic patients and animals (Aveleira 2009). AGEs operating via cell surface receptors can be formed from prolonged hyperglycemia, which in turn cause cellular dysfunction and diabetic complications. The main targets for AGE toxicity are the retinal capillaries, which may lead to the apoptosis of pericytes. In addition, it has been shown that AGEs stimulate NFκB directly in vascular smooth muscle cells (VSMCs), resulting in cell damage (Patel & Santani 2009).

1.3.1.4. Oxidative stress

Oxidative stress due to the formation of ROS is directly associated with the progression of vascular complications of diabetes (Aveleira 2009). The production of ROS increases in hyperglycemia, causing activation of PKC and polyol pathways, as well as the production of AGEs. Indeed, vascular damage and lipid peroxidation are known to result from the formation of ROS, nitric oxide and hydrogen peroxide. The retina has a high glucose and oxygen absorption capacity and contains polyunsaturated fatty acids, with available literature demonstrating that it is these characteristics that expose the retina to damage related to oxidative stress. Elevated levels of oxidative stress markers, such as

thiobarbituric acid-reactive substances (TBARS), have been observed in the diabetic rat (Aveleira 2009). Moreover, hyperglycemia leads to increased oxidative stress, which in turn produces an elevated level of isoprostanes and prostanoids (Balasubramanyam *et al* 2002). Then, thromboxane prostanoid receptors are activated, which are found on the walls of blood vessels and in platelets. The activation of thromboxane prostanoid receptors causes inflammation and damage in the circulatory system. During hyperglycemia, the oxidative stress pathway causes an excessive production of superoxide, which is in turn connected to biochemical pathways such as the production of ROS involved in diabetic retinopathy. Consequently, oxidative stress resulting from hyperglycemia may be one of the main reasons for the excessive production of superoxides through the mitochondrial electron transport chain (ETC) (Balasubramanyam *et al* 2002). Excessive production of superoxide anion, according to Balasubramanyam (2002), initiates ROS and oxidative stress in diabetes.

Studies in rats show increased levels of superoxide in cells of the retina that were incubated in high glucose and H₂O₂ (Tarr *et al.* 2013). In addition, VEGF is a growth factor that is associated with DR. There are two pathways, a calcium influx channel and a mitogen activating protein kinase signaling pathway are induced when VEGF binds to the membrane receptors. This activation causes a breakdown of the retinal barrier and leakage of vascular products. Therefore, anti-VEGF agents, such as ranibizumab and bevacizumab, can be used for the treatment of complications of DR (Tarr *et al.* 2013).

1.3.1.5 Hexosamine pathway activation

During glycolysis, glucose is converted into glucose-6-phosphate, which is converted to fructose-6-phosphate. The hexosamine pathway is initiated when glutamine fructose-6-phosphate amidotransferase (GFAT) converts fructose-6-phosphate into N-acetylglucosamine-6-phosphate, precipitating a downstream reaction whereby N-acetylglucosamine-6-phosphate metabolizes into uridine diphosphate

(UDP)-N-acetylglucosamine (UDP-GlcNAc) (as shown in Fig 3) (Aveleira 2009). Furthermore, in hyperglycemia, the flow of glucose *via* the hexosamine pathway increases, resulting in insulin resistance (Aveleira 2009). Researches have shown that the activity of GFAT is enhanced in T2DM and the expression of GFAT also changes in DR (Balasubramanyam *et al* 2002). This study further assumes that the GFAT is found in the tissues that are critical to the progression of diabetic complications; however, to date no evidence exists to show the presence of GFAT in eye tissues. It is suggested in the literature that high glucose concentration stimulates the hexosamine pathway, which in turn causes several shifts in protein function and/or gene expression, leading to progression of pathogenesis of diabetes complications (Balasubramanyam *et al* 2002).

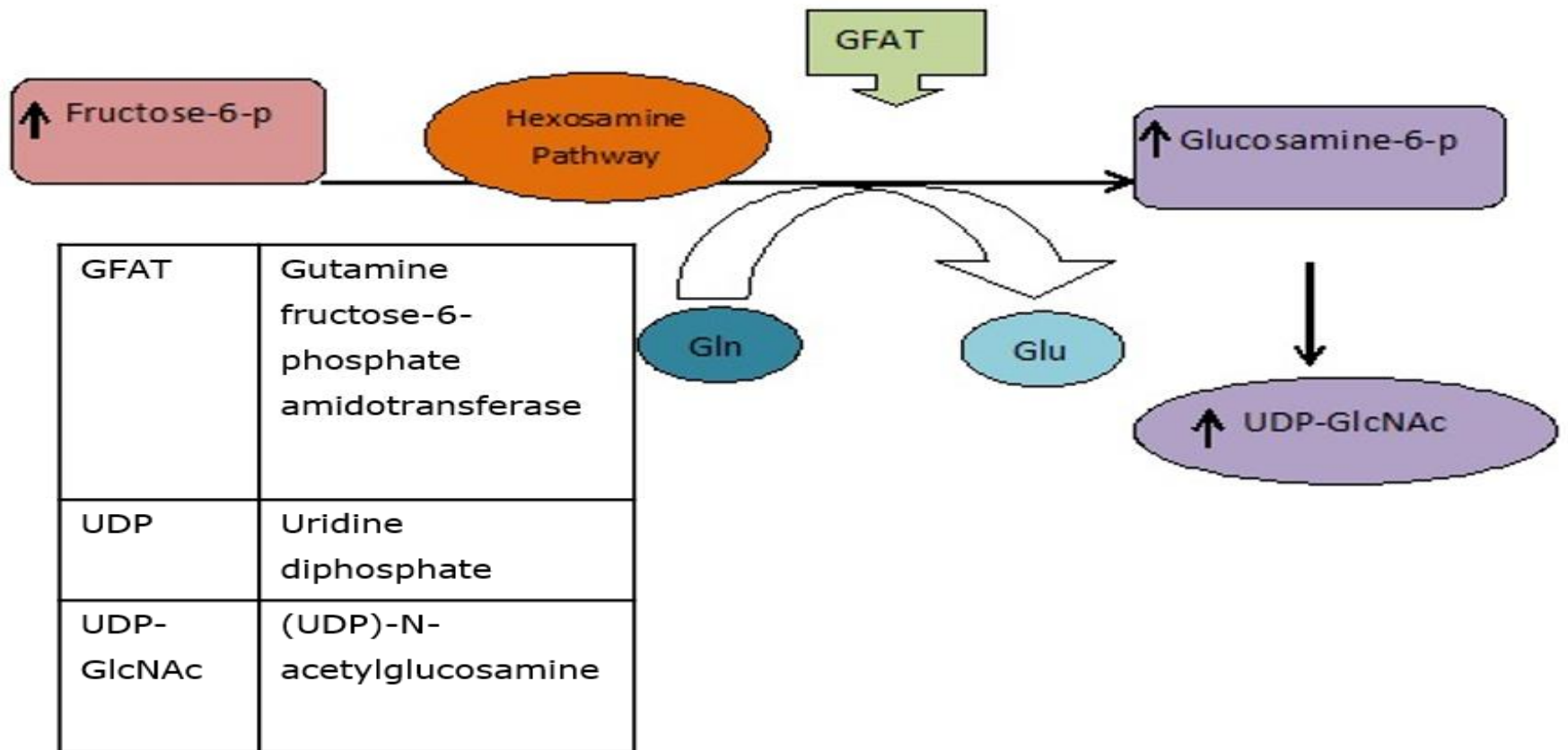


Figure 3: Hexosamine Pathway, hyperglycemia increases the flux of fructose-6-phosphate into hexosamine Pathway. GFAT converts fructose 6-phosphate to glucosamine 6-phosphate, adapted from Alghadyan (2011)

1.4 Nuclear factor kappa B

1.4.1 The relationship between *NFκB* and diabetes

NFκB is a transcription factor, which plays an intrinsically important role in the regulation of different genes and proteins in the inflammatory response, including cytokines such as Tumor Necrosis Factor-α (TNFα) and Interleukin-1β (IL-1β) (Chakrabarti 2007). NFκB consists of five polypeptide subunits including p50, p52, RelA (p65), C-Rel and RelB. It is also regulated by inhibitors that include IκBα, IκBβ, IκBγ and Bcl-3 (Figure 4) (Chakrabarti 2007).

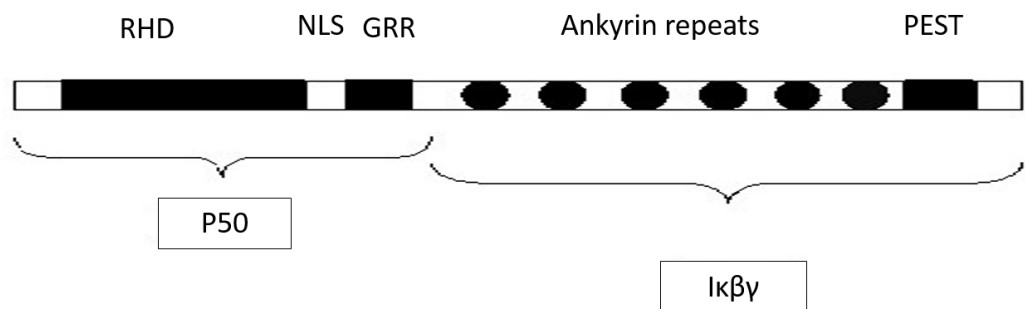


Figure 4: Human NFκB1 Structure, Adapted from Chen 2014

NFκB1 gene produces a protein consisting of 968 amino acids with molecular weight of 105 KD. In the N-terminal region, which contains serine residues and Rel homology domain (RHD). RHD has 300 amino acids that important for DNA binding and interaction with IκB proteins. The C-terminal has ankyrin repeats are found in the IκB family members including IκBa, IκBb and IκBe (Chen 2014). GRR is a glycine-rich region, which is in the region 375 to 400 of NFκB, and it is important for guiding the NFκB1 cleavage.

Whereas, various copies of ankyrin repeats are located in the C-terminal region and it can be found in I κ B family members. Phosphorylation occurs at Ser-903 and Ser-907 primers p105 and this is in response to TNF- α activation (GeneCards 2013).

There are some studies that show that during ubiquitination of the proteasome, NF κ B1 is cleaved to make the p50 molecule. Additional studies proposed by Lin (1998) and Ghosh (Sankar *et al.* 1998) show that the glycine-rich region (GRR) is important to guide cleavage of NF κ B1 (Chen 2014).

Through acting via nuclear localisation sequences (NLSc), I κ B proteins can retain NF κ B dimers in the cytoplasm (Patel & Santani 2009). By I κ B kinase (IKK) complex, the phosphorylation of cytoplasmic I κ B begins, leading to activation of NF κ B. The NF κ B heterodimers discharge to the nucleus after degradation of I κ B through proteosomal system. Subsets of genes are stimulated due to binding of NF κ B heterodimers to nuclear DNA (Chakrabarti 2007).

NF κ B is induced when free fatty acids bind to TLRs. This activation causes insulin receptor substrate-1 (IRS-1) phosphorylation via JNK and PKC. This change can lead to a down regulation of glucose transporter GluT-4 and leads to insulin resistance (Paneni *et al.* 2013).

There are two activation pathways for NF κ B, namely the classical pathway and the alternative activation pathway (Figure 5). In the classical signalling pathway, phosphorylation of I κ B proteins occurs through and initiated by I κ B kinase (IKK) complex, causing polyubiquitination at sites of I κ B α , which then leads to degradation through 26S proteasome. Afterwards, free NF κ B dimers discharge. The important component for signalling through the classical pathway is IKK β . The classical pathway is also activated through binding of a ligand to the B-cell receptor (BCR), T-cell receptor (TCR) or toll-like receptor. Through this pathway, transcription of the target genes occurs which encode cytokines, chemokines and adhesion molecules (Nishikori 2005) all of which have been implicated in DR. The alternative pathway, NIK, which is also known as NF κ B inducing kinase,

stimulates IKK α homodimer (IKK β and IKK γ) and leads to phosphorylation of p52 at two C-terminal sites through IKK α homodimer. Afterwards, ubiquitination and degradation causes the release of p52 (Nishikori 2005). Extant literature demonstrates that this pathway is activated through stimulation of TNF receptor, the receptor lymphotoxin- β receptor (LT β R) and B-cell activating factor, including CD40 and CD30 (Nishikori 2005). The stimulation of this pathway is responsible for controlling the adaptive immune system and lymphoid organ development (Nishikori 2005). In addition, activated NF κ B complex binds to DNA at κ B binding motifs like 5'-GGGRNNYYCC-3' where R is Adenine (A) or Guanine (G) and Y is a Cytosine (C) or Thymine (T). Phosphorylated I κ B generated from NF κ B/I κ B complex in turn lets NF κ B molecules translocate into the nucleus (Romzova *et al.* 2006). Then, transcription is stimulated through binding NF κ B molecules with the consensus sequence (5'-GGG-ACTTCC-3') of several genes (Romzova *et al.* 2006).

NF κ B1 and NF κ B2 known as large precursors, which are p105 and p100. These large precursors can generate the mature NF κ B subunits p50 and p52. NF κ B1 (p105) is cleaved to make the p50 during the ubiquitination process (Patel & Santani 2009). P52 is generated from p100. P50 and p52 as homodimers work as transcriptional repressors when they bind to κ B elements. In addition, NF κ B has two subunits that can exist as homodimers (p50/p50) or heterodimers (p65/p50). Homodimeric complex created by two identical molecules and a heterodimeric complex created by two different macromolecules. The Rel-like domain, which containing proteins that consist of homodimer and heterodimer set up from at least five subunit such as RelA/p65, RelB, NF κ B1/p50, c-Rel and NF κ B2/p52. Each subunit has various characteristic of DNA binding. For instance, the p50 homodimer is responsible for repression of gene transcription. Whereas, the p65/p50 heterodimer is recognized as an activator of gene transcription (Patel & Santani 2009). The heterodimers RelB/p52 and p50/p65 are transcriptional activators of the NF κ B gene that promotes gene transcription *via* binding to κ B DNA. Binding of homodimers of the p50 or p52 inhibits the transcription of the NF κ B gene. RelA (p65)/p50 is

found in the classical pathway when activated by TNF- α and IL-1. Degradation of p100 forms the active p52 and it is available during the alternative pathway. NF κ B-inducing kinase (NIK) activation of IKK α , results in the phosphorylation and processing of p100 and the formation of p52/RelB (Patel & Santani 2009).

Evidence from the literature demonstrates that there is a central role played by NF κ B in the retina. Patel and Santani (2009) state that "...retinal NF κ B is activated early in diabetes and remains activated for up to 14 months." It was noted that diabetes has important effects on NF κ B, which leads to the movement of p65 subunits and p50 subunits to the nucleus of retinal pericytes and to the nucleus of retinal endothelial cells, respectively (Chakrabarti 2007). The expression of pro-inflammatory factors including cytokines such as TNF α are also regulated through stimulation of NF κ B, resulting in elevated levels of other cytokines, for example IL-1 β , IL-6 and IL-8.

In the case of DR, AGEs are irrevocably generated and they accumulate within the retinal capillary cells, with academics and medical practitioners postulating that more ROS are generated via the AGE pathway to cause the activation of NF κ B and eventually cause further damage to the cells (Patel & Santani 2009). Consequently, patients with proliferative diabetic retinopathy and also diabetic rats have elevated levels of cytokines in their vitreous fluid (Nehme & Edelman 2008). Extant literature also demonstrates that "...the levels of IL-1 β are also substantially increased in retinal capillary cells incubated in high glucose media" (Patel & Santani 2009).

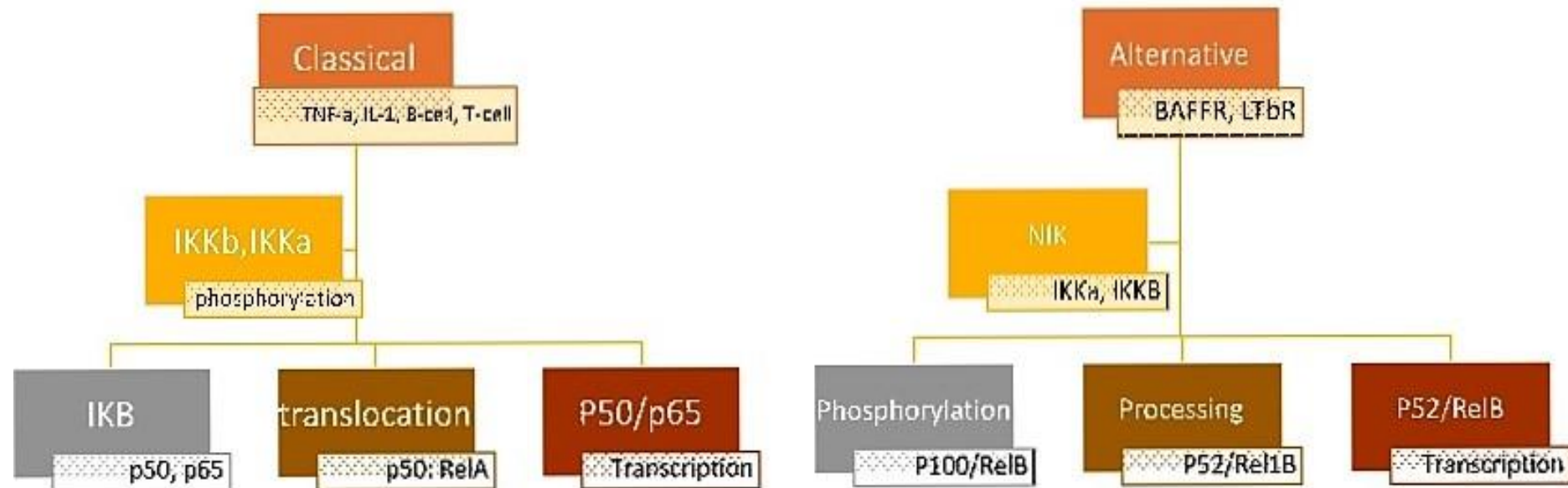


Figure 5: Classical and Alternative Pathways of NFκB, adapted from Patel and Santani (2009)

Figure 5 illustrates both the classical and alternative signaling pathways of NFκB activation: (Classical) external signals such as TNF-α, IL-1, B-cell and T-cell receptor stimulate the classical pathway and the phosphorylation of IKβa, resulting in the degradation of Iκβa by proteasome. These reactions encourage translocation of p50: RelA to the cytoplasm, the alternative pathway involves NIK activation of IKKa, resulting in the phosphorylation and processing of p100 and the generation of p52: RelB heterodimers (Patel & Santani 2009).

Experiments have shown that activated NFκB found in the retina following exposure to high glucose concentration causes movement of p65 into the nuclei of pericytes, endothelial cells and ganglion cells (Zhang *et al* 2011; Rohilla *et al* 2012). Indeed, one particular experiment conducted using the DNA binding technique demonstrated that NFκB DNA binding activity increased in endothelial or pericyte cells of the retina (Zhang *et al* 2011; Rohilla *et al* 2012). Evidence from mRNA and immunohistochemical analysis showed that the expression of NFκB increased in epiretinal membranes of diabetic retinopathy patients (Zhang *et al* 2011; Rohilla *et al* 2012). Moreover, single nucleotide polymorphisms (SNPs) were identified which were thought to have a role in diabetes (Ensemble, 2013). Therefore, polymorphisms were investigated in this study, using a bioinformatics approach through computational analysis.

HIF1 is another important transcription factor that is controlled by hyperglycemia. There are several studies showing that, HIF1α level is decreased in diabetic patients cells and in cells that are cultured in high glucose medium (25mM) (Gao *et al.* 2007). During glycolysis, HIF1 controls the enzymes that are required during this process and, which can moderate cellular glucose uptake (Xiao *et al.* 2013). The main role of HIF1 is the sensing of low oxygen levels in the cell. It is composed of two subunits: HIF1α which is stabilised by O₂ insufficiency and is continually expressed HIF 1 beta (Semenza 2001). In addition, HIF1α has been shown to be mediated in high glucose concentrations (Catrina *et al.* 2004).

1.5 Rationale for study

The research in this project was carried out to investigate genetic polymorphisms within the NFκB1 gene. Also, to examine the role of this specific inflammatory mediator in the progression of diabetes using the response of U937 cells to different glucose concentrations and H₂O₂.

The initial approach of this study was to investigate NFκB as it has a prominent role in diabetes and in particular DR. Bioinformatics was used to determine SNPs by analysing the genetic background of patients with diabetes. It has been shown that there is a connection between the polymorphisms of NFκB1 promoter regions and diabetes (Song *et al.* 2011). Therefore, this study screened SNPs within the NFκB1 gene locus and chose relevant SNP sites.

Investigation of genetic polymorphisms is an approach, which can be used to study rare variants within a gene, and was used in this study. Some SNPs have several effects and induce several changes to occur. In addition, some of the SNPs, which are located in coding regions, can damage the protein structure and overall size and, thus, alter protein function. This alteration also can effect protein expression (Tadhg, 2006). Also, promoter activity can be affected when SNPs occurred in 5' regions. SNPs in 3' (UTR) regions can influence mRNA stability. Therefore, SNPs can lead to the alteration of gene function and can affect a transcript. The alteration of gene expression may lead to disease. Additionally, repeat polymorphisms that are located in 5' of human insulin gene can cause diabetes (Tadhg, 2006).

In order to identify a SNP of interest the first part of this study uses bioinformatic search protocols. The second part of this study was to investigate the SNP of interest using specific restriction enzymes. Finally, the effect of NFκB and HIF1α mRNA expression in response to different glucose was also carried out in response to oxidative stress. The finding of this study is highlighted as novel, as no one has examined the gene databases to identify the SNP rs230539 in NFκB before in U937 cells.

Chapter 2:
Materials and Methods

2.1. Materials

All chemicals were purchased from Sigma-Aldrich, UK and all cell culture reagents were obtained from Gibco, UK unless otherwise specified.

The human U937 cell line used in this study was purchased from the European Collection of Cell Cultures (Cat no. 85011440, ECACC, Public Health England, UK). U937 cells were derived from malignant cells of a pleural effusion from a 37-year-old Caucasian male with a diffuse histolytic lymphoma, which expresses many monocytic-like characteristics. U937 cells are a good experimental tool for use in the examination of monocytic cell function. The U937 cells were pre-differentiated cells.

2.2. Methods

2.2.1 Bioinformatics

A range of *in silico* analysis tools were used to explore the current genetic information available regarding the human NFκB1 gene. The websites used for the bioinformatics analysis in this study are listed in Table 1.

Table 1: Bioinformatics websites used for in silico analysis

Name of bioinformatics analysis	Website URL ^a
The Ensemble genome browser	http://www.ensembl.org
National Centre for Biotechnology Information (NCBI)	http://www.ncbi.nlm.nih.gov/snp
Primer Quest	http://eu.idtdna.com/PrimerQuest/Home
NetPhos 2.0	http://www.cbs.dtu.dk/services/NetPhos/
Nebcutter	http://tools.neb.com/NEBcutter2/

^a Websites used to explore genetic information of human NFκB1 gene and for the identification of sequences of human NFκB1 gene, the design of primer sequences, the identification of potential phosphorylation sites and the location of restriction sites within the amplified sequence.

The Ensemble genome browser is a collection of genome databases for vertebrates and other species whilst, the National Centre for Biotechnology Information (NCBI) (National Center for Biotechnology Information. 2012) provides access to biomedical and genomic information. These resources were used to identify the sequence of the human NFκB1 gene, to locate highly conserved regions within the gene and to review known NFκB1 sequence variants that may be linked with diseases, such as, diabetes. Primer Quest (Primer quest. 2013) programme is a tool used for designing primers for PCR and sequencing. The programme NetPhos was used to identify the phosphorylation sites and to show predictions for serine, threonine and tyrosine phosphorylation sites for proteins. Nebcutter tool (Vincze *et al.* 2014) was used to determine the sites of restriction enzymes through providing a DNA sequence analysis.

Ensemble (2013) was used as follows: The species was selected as 'Human' and then the name of the gene 'NFκB1' was typed into the search bar. The search was started by clicking on the 'Go' button followed by 'Gene' which reveals a variety of information about the gene including, gene ID, genomic location, transcripts and sequence variations. Also, the Ensemble website provides an option for a 'Map view', which shows chromosomal diagrams and single nucleotide polymorphism (SNPs). In addition, the gene region display provides the intronic and exonic regions and the untranslated regions (UTR) in relation to the position of a SNP. The genetic information can be created in a graphical display format, which presents mapping of the SNPs over the genetic sequence.

As an alternate presentation the format of the sequence was also converted to a text based format (FASTA) and the programme NetPhos 2.0, was used to identify phosphorylation sites to determine potential protein regulatory sites associated with SNPs. NetPhos was used as follows:

The sequence in FASTA format was pasted into the input field and "submit the job" was selected. Then, the programme ran and displayed the output in the browser window.

NCBI was used to obtain the FASTA sequence which is the text based format used to represent a nucleotide sequence that could then be used with Ensemble to calculate protein function prediction *via* Sorting Intolerant From Tolerant software (SIFT) and Polymorphism Phenotyping tool (PolyPhen- V2). SIFT shows the effect of an amino acid replacement on protein function which depends on the amino acid physical properties and sequence homology. Polymorphism Phenotyping (PolyPhen) is a tool, which can be used to show the effect of an exchange of nucleotides on the structure and function of human proteins. Therefore, predicting the impact of the SNP on protein function and structure can be calculated by using these tools. The calculation was preceded by providing a score and a qualitative prediction (probably damaging, possibly damaging, or unknown).

Using the Ensemble programme, a specific SNP of interest was identified for further study. The region of interest was then analysed using the programme Primer Quest (Primer quest. 2013) to generate specific primers that would span the identified region of interest. This was followed by a BLAST ran of the sequences selected to ensure specificity of the DNA regions. New England Biocutter programme was then used to identify restriction enzyme sequences within this region that could be used to further distinguish the SNP of interest.

2.2.2 Cell culture and cell counting

U937 cells were cultured in Roswell Park Memorial Institute (RPMI-1640) medium with 2 mM L-glutamine, supplemented with 100 µg/mL streptomycin, 100 U/mL penicillin and 10% (v/v) heat inactivated foetal bovine serum (FBS). The cell suspension was centrifuged at 10,000 g (HERA Cell 150, Heraeus/Thermo Fisher Scientific/Kendro, UK) for 5 minutes. After centrifugation, the supernatant was removed and the pellet resuspended in 1 mL RPMI medium. The cells were counted using a Neubauer haemocytometer and 1 million cells transferred to a T-25 (25 cm²) culture flask with 5 mL RPMI medium. The cultured cells were

incubated in an incubator at 37°C, with 5% CO₂ (HERA Cell 150, Heraeus/Thermo Fisher Scientific/Kendro, UK). After four days, U937 cells were counted and transferred to a 6 well plate (1 × 10⁴ cells/well) for experiments as detailed below.

In brief, a 50-μL aliquot of cell suspension was gently mixed with 0.4% (v/v) of Trypan blue dye (1:1 dilution) and added to the haemocytometer. Trypan blue was used to visualise viable and non-viable cells, which appear clear and blue, respectively. Non-viable cells appear blue because of the increased permeability of the plasma membrane. The cells were viewed under a microscope at 100x magnification (Leica, Leica Microsystems, UK) and the number of cells in the outside four squares counted. The cell number was determined using Equation 1.

Equation 1:

$$\boxed{\text{Number of cells/ml} = \text{number of cells counted} \times \text{dilution factor} \times 10^4}$$

After counting, the cells were seeded and grown in 6-well plates. Multiple plates were used to allow for the incubation of U937 cells at the following time intervals: 0, 30, 60 and 180 minutes, with and without hydrogen peroxide (H₂O₂ 10 μM) at 37°C, with 5% CO₂. In addition, 1x10⁷ U937 cells were grown in different glucose concentrations (5.5 mM, 20 mM and 40 mM) and incubated for 24 hours at 37°C, with 5% CO₂.

2.2.3 DNA extraction and purification

DNA extraction was carried out using the PeqLab mini kit according to the manufacturer's instructions (peqGOLD Tissue DNA Mini Kit, PEQLAB_v0912, PeqLab, UK). Proteinase K (25 mg) and RNase A (10 mg) were provided as powders and were dissolved, before use, by vortexing in TE (Tris EDTA (Ethylenediaminetetraacetic acid)) buffer (10 mM Tris, pH 8.0, 1 mM EDTA). For Proteinase K, 1.25 mL TE buffer was added to 25 mg to give a final concentration of 20 µg/µL and was stored at -20 °C in 50 µL aliquots, until required. For RNase A, 500 µL TE buffer was added to 10 mg to give a final concentration of 20 µg/µL. The RNase A solution was then stored in 50 µL aliquots at 4°C, until required.

Cells grown in 6 well plates were collected and centrifuged. After centrifugation, the cells were retained and the supernatant was discarded. DNA lysis buffer (400 µL) was added to the U937 cell pellet and mixed by pipetting up and down. Proteinase K (20 µL) was firstly added to cells, the contents of the tube was gently mixed, then 15 µL RNase A was added and the contents of the tube mixed again by pipetting up and down. The samples were incubated at 50°C for 30 minutes and mixed 4 times during the incubation by vortexing for 10 seconds. After incubation, 200 µL DNA binding buffer (which contains a chaotropic salt) was added and mixed by pipetting and vortexing. A Perfectbind DNA column was placed in a collection tube and the sample (750 µL) loaded onto the column. The Perfectbind DNA column with the collection tube was centrifuged (Eppendorf 5415 D centrifuges, UK) for 1 minute at 10,000 g. The column was kept and the flow-through was discarded. DNA Wash buffer (650 µL) was added to the column and centrifuged for 1 minute at 10,000 g. The flow-through was discarded and the washing step was repeated three times. After the flow-through was discarded for the third time, a new collection tube was used and centrifuged for 2 minutes at 10,000 g (thus, this was the drying step). Then, Elution buffer (200 µL; 10 mM Tris-HCl, pH 9.0) was added to the column and incubated for 3 minutes at 70°C. Then, the sample was

centrifuged for 1 minute at 6,000 g (thus, this was the elution step). The eluent contained the DNA so this tube was not discarded.

Finally, genomic DNA was collected in an Eppendorf tube (100 μ L+ 100 μ L = 200 μ L total final volume). DNA concentration was measured by diluting the sample 1:10 and using a spectrophotometer (BioMate 5 spectrophotometer, Thermo Scientific, USA) set at 260 nm and 280 nm. The 260/280 nm ratio was determined and the final concentration of DNA recorded since the amount of UV absorbed by the DNA solution at 260 nm is directly proportional to the amount of DNA in the sample where a optical density unit of 1 is equal to 50 μ g/mL DNA. The concentration of DNA in each sample was determined using Equation 2.

Equation 2:

$$\text{Concentration } (\mu\text{g/mL}) = (\text{A}_{260} \text{ reading}) \times \text{dilution factor} \times 50 \mu\text{g/mL}$$

2.2.4 Polymerase chain reaction (PCR)

The SNP of interest was selected and amplification of the region of DNA containing the selected SNP was carried out using genomic DNA (gDNA) from U937 cells. The amplification was carried out with specific primers (Table 2). That would generate a product of 206bp.

Table 2: NFκB Forward and Reverse Primers used in PCR.

	Length of primer	Tm (Melting Temperature, °C)	GC % (Self Complementarity)	Seq (Primer Sequence, 5'→3')
Forward	24	62	45.8	CAGAGAGACCAGAGAAACCTTTAC (Sense)
Reverse	22	62	45.5	GAGTGCTGTGTGTGAGGAAATA (antisense)

Master mix (25 µL) contained RedTaq, 0.2 µM Forward Primer, 0.2 µM reverse primer and H₂O. The samples were placed in a thermocycler (Biometra T3000 thermocycler, Germany) with cycling conditions as follows: denaturation at 94°C for 1 minute, annealing at 56°C for 2 minutes and elongation at 72°C for 3 minutes (for a total of 30 cycles).

2.2.5 Gel electrophoresis

Agarose gel electrophoresis was used to determine the size of DNA fragments and for analysing amplified DNA bands. The gel was prepared using electrophoresis grade agarose (Invitrogen, Life Technologies, USA) at a concentration of 1.8% (w/v) in Tris-Borate-EDTA buffer (1×TBE) procedure was followed according to the manufacturers' protocol. Agarose was measured (0.99 g) and 1×TBE buffer (55 mL) added. The mixture was heated using a microwave for 1 min until the solution appeared clear and without bubbles. Then 2 µL of gel red nucleic acid stain was added, and gently mixed. The comb was placed into the gel mold on one end. The melted agarose mixture was poured into the gel mold. After the gel had cooled and solidified, the gel mold was inserted into the gel tank, covered with 1×TBE buffer and the comb removed which left empty wells for addition of the samples.

Samples (5 µL) of the amplified DNA and fragments of known sizes (HyperLadder 100bp, Bionline, UK) were loaded onto the gel and

electrophoresis ran at 80V for 1 hour. DNA fragments were then visualised using the Fusion X7 (Peqlab, UK) and an image of the gel retained. DNA fragment sizes were then determined by comparison with the distance migrated by DNA of known size. The distance migration was measured *via* using a ruler. A table for each gel was created, which contained the ladder fragments (bp), the fragment log (log 10 base pairs) and the migrated distance (in cm). Then, excel was used to create a scatter graph. The fragment log was plotted on the y axis and the migrated distance plotted on the x axis. Next, a straight line was created and the equation of the straight line used to determine the size of the DNA fragments.

2.2.6 Restriction digest

Digestion of the PCR products was done using specific restriction endonucleases. The New England Biolabs (NEB) cutter software V2.0 (Table 1) was used to find specific restriction enzymes to digest rs230539 sequence as shown in Figure 6.

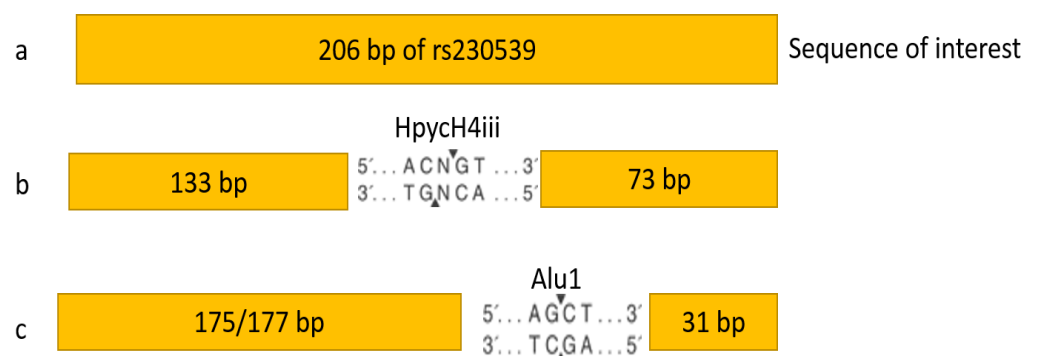


Figure 6: Restriction Enzymes (adapted from Vincze et al., 2014) which can be used to digest PCR products for a region of 206 bp of rs230539.

(a) A region of 206 bp of rs230539 was analysed for specific restriction enzyme sites using NEB cutter software. The two sites identified are for (b) HpyCH4III and (c) Alu1.

A number of enzymes were found to cut the DNA sequence of the PCR product. The enzyme HpyCH4III (TaaI) was found to cleave at the SNP site generating products of 133 bp and Alu1 restriction enzyme cleaves the PCR product at position 175 predicting that 2 fragments of 175 bp and 31 bp should be visible.

PCR products were digested by the enzyme HpyCH4III (New England BioLabs, UK), for one hour, 4 hours or overnight at 37°C. This enzyme should cleave the AC N GT site and the fragment length was analysed on a 1.8 % (w/v) agarose gel (prepared as described in Section 2.2.5). Digestion of rs230539 region was carried out in a total volume of 20 µL: using 5 µL of PCR product with 1 µL endonuclease HpyCH4III (refer to Table 3 for details). In addition, two other restriction enzymes Alu1 and PvuII (New England BioLabs, UK) were tested for digestion of rs230539 region. Digestion was carried out in a total volume of 20µL as mentioned in Table 3. Samples were incubated at 37° C for 1 hour and resolved using agarose gel electrophoresis as previously outlined in Section 2.2.5.

Table 3: Samples prepared for digestion (5 sample, un cut, with Hpych4iii, with AluI and with PvuII)

Sample No.	PCR reagent	Enzyme	Buffer	Water (total 20 μ l)
1 (-ve)	5 μ l	-	2 μ l (cutsmart, 100 buffer)	13 μ l
2	5 μ l	1 μ l (of Hpych4iii)	2 μ l (cutsmart, 100 buffer)	12 μ l
3	5 μ l	1 μ l (of Alu1)	2 μ l (cutsmart, 100 buffer)	12 μ l
4 (-ve)	5 μ l	-	2 μ l (of 3.1 buffer)	13 μ l
5	5 μ l	1 μ l (of PvuII)	2 μ l (of 3.1 buffer)	12 μ l

2.2.7 PCR purification

The Qiagen MinElute Reaction Cleanup Kit (Qiagen, UK) was used to purify the amplified DNA from enzymes, salts and primers. The protocol was carried out according to the manufacturers' procedure. Briefly, 5 volumes of Buffer PB (binding buffer, 5 M Gu-HCl and 30% isopropanol) to 1 volume of the PCR sample were added together, therefore, 225 μ L of Buffer PB was added to 45 μ L of PCR sample (with primer concentration, 0.2 μ M). The colour of the mixture was violet, therefore 10 μ L of sodium acetate, pH 5.0 was added to turn the colour of the mixture to a yellow colour and procedure was followed according to the manufacturers' protocol. QIAquick spin column was placed in a 2 mL collection tube. The sample was applied to the QIAquick column and centrifuged (Eppendorf 5415 D centrifuge, UK) for 30 seconds at 17,900 g. Flow-through was discarded and the QIAquick column was placed back into the tube. Buffer PE (0.75 mL) was added (according to the manufacturers' procedure) to the QIAquick column and centrifuged at 17,900 g for 30 seconds. Flow-through was discarded and QIAquick

column was placed back into the tube. The column was centrifuged at 17,900 g for one minute and transferred to a clean 1.5 mL centrifuge tube. Buffer EB (50 μ L) (10 mM Tris·Cl, pH 8.5) was added to the membrane of the QIAquick column and centrifuged at 17,900 g for 1 minute.

2.2.8 Sequencing

DNA samples and primers were sent to the College of Life Sciences, University of Dundee, UK, for sequencing. Primer concentration required to be sent for sequencing was 3.2 μ M along with 20 ng PCR product. The similarity between two sequences was done *via* comparing the predicted sequence and the sequence of the PCR product.

2.3 RNA extraction and purification

2.3.1 RNA extraction using RNeasy mini kit

U937 cells were incubated in six well plates (maximum of 10^7 cells per well). Cells were collected in individual Eppendorf tubes and centrifuged at 10,000 g (Eppendorf 5415 D centrifuge, UK) for 15 minutes (at 4°C). The supernatant was removed from each tube and the cell pellet stored on ice until all samples were collected. Ice cold Phosphate Buffered Saline (PBS) (1 mL) was added to the cell pellet and the cells were gently resuspended, and re-centrifuged at 10,000 g for 10 minutes. The supernatant was removed and discarded. This washing step was repeated three times and the supernatant removed after each wash. RNALater (Invitrogen, UK) (1 mL) was added to the cell pellet. RNALater is an RNA stabilisation solution used to stabilise and keep RNA in an intact form. The sample was gently pipetted up and down to ensure all cells within the pellet were exposed to RNALater. All samples were stored at -20°C, until required.

RNA was extracted by using the RNeasy mini kit (Qiagen, UK, Cat No 74104). The methodology for RNA extraction was followed as stated in the manufacturer's protocol. Briefly, a 300 μ L aliquot of 70% (v/v) ethanol was added to the cell pellet and mixed by pipetting. The homogenised sample (500 μ L), including any precipitate, which was formed on addition of ethanol, was added to an RNeasy spin column which was placed in a 2 mL collection tube. The tubes were centrifuged (Eppendorf 5415 D centrifuge, UK) at 8,000 g for 15 seconds to bind the RNA onto the column and the flow-through discarded after centrifugation. Washing buffer (RW1; 750 μ L) was added to the spin column and centrifuged at 8,000g for 15 seconds. Ethanol was added (44 mL of ethanol added to obtain 55 mL RPE buffer) to the RPE buffer (concentrated wash buffer used for washing membrane bound RNA) and this was then added and centrifuged at 8,000 g for 15 seconds. The wash step was repeated by the addition of 500 μ L RPE buffer and centrifuged at 8,000 g for 2 minutes. The flow-through was discarded each time. The column was then placed in a fresh 2 mL collection tube and centrifuged at 8,000 g for 1 minute to dry the columns from any carryover of RPE buffer. Finally, the spin column was placed in a 1.5 mL collection tube and 50 μ L RNase free water (elution buffer) added directly on to the RNeasy membrane. The tubes were centrifuged at 8,000 g for 1 minute to elute RNA. The samples were ready to be used immediately or stored at -20°C until required. The concentration of RNA was measured by using a spectrophotometer at an absorbance of 260 nm. The solution was diluted (1:20) in Diethylpyrocarbonate (DEPC) treated water.

20 μ L RNA + 380 μ L DEPC dH₂O

The concentration was calculated using Equation 3:

$$A_{260} \times \text{dilution factor} \times 40 = X \text{ } \mu\text{g/mL RNA concentration}$$

2.3.2 RNA extraction using TRIzol reagent

An alternate method of RNA extraction was also used. Total RNA was extracted from 1×10^7 U937 cells. U937 cells were homogenised in 1 mL TRIzol reagent (Sigma, UK) (which is a phenol-based solution) for 5 minutes at room temperature (RT). Chloroform (200 μ L; minimum grade 99%) was then added and the phases separated by centrifugation (PK121R centrifuge, ALC International, Italy) for 15 minutes at 17,900 g at 4°C. The RNA (present in the upper phase) was transferred to a fresh Eppendorf tube and incubated with 500 μ L of Isopropyl alcohol (propan-2-ol, Fisher Scientific, UK) at RT for 10 minutes to allow for RNA precipitation. After centrifugation for 10 minutes, at 12,000 g, the RNA pellet was washed with 500 μ L of 75% (v/v) ethanol and then dissolved in 20 μ L DEPC treated water. The concentration of RNA was measured by using a spectrophotometer at an absorbance of 260 nm (Table 4).

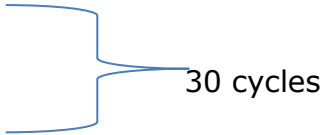
Table 4: RNA concentration for 1×10^7 U937 cells for loading of 1 μ g and 2 μ g of the sample

Sample	RNA Concentration (μ g/mL)	RNA Concentration (μ g/1000 μ L)	Volume of RNA (μ L)	Volume of H ₂ O required (made up to up to 12 μ L)	Volume of loading dye required (μ L)
10^7 (sample1) (1 μ g)	2432	2.432	$1/2.432=0.4$	9.6	2
10^7 (sample2) (2 μ g)	2432	2.432	$2/2.432=0.8$	9.4	2

2.4 cDNA synthesis and reverse transcriptase polymerase chain reaction (RT-PCR)

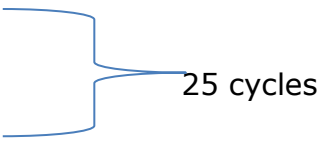
RNA (4 µg) extracted using TRIzol reagent was reversed transcribed in a total volume of 20 µL, using Tetro cDNA synthesis kit (Bioline, UK) using oligo dT primers and following the procedure according to the manufacturer's instructions and ran on a Biometra thermocycler (T3000 Thermocycler, Biometra, UK). All samples were incubated at 45°C for 30 min, when using oligo dT primers. Then, the reaction was terminated by incubating at 85°C for 5 min, and chilled on ice. All samples were then stored at -20°C until required.

Moreover, the PCR was run with 0.2 µM NFκB and 0.2 µM HIF1α primers as follows:

- a. 94°C for 2 minute.
 - b. 94°C for 50 Sec.
 - c. 60°C for 1 minute. Annealing Tm
 - d. 72°C for 2 minutes.
 - e. 94°C for 50 sec.
 - f. 60°C for 1 minute.
 - g. 72°C for 2 minutes.
 - h. 4°C.
 - i. Transferred for storage at -20°C.
- 

These samples were analysed on a 1.8% (w/v) agarose gel ran at 80V for one hour.

Modified conditions were used with β 2- microglobulin (1 μ M) for a total of 25 cycles and was conducted as follow,

- a. 94°C for 4 minute.
 - b. 94°C for 1 minute.
 - c. 59°C for 2 minute. Annealing Tm
 - d. 72°C for 2 minutes.
 - e. 72°C for 8 minutes.
 - f. 4°C.
 - g. Transferred for storage to -20°C.
- 
- 25 cycles

The samples (5 μ L) and ladder (2 μ L) were run on a 1.8% gel, at 80 V for half an hour.

cDNA was amplified using β 2- microglobulin and β -Actin as internal controls, HIF1- α and NF κ B primers with Red TaqMan Universal PCR master mix (containing Redtaq, forward primer and reverse primer and H₂O), PCR reagent (total 50 μ l) in primer concentration 0.2 μ M per primer. The details of the primers used are in Table 5.

Table 5: Details of primers used for PCR. The table illustrates the primers used for cDNA amplification, which are HIF1 α , NF κ B, β -Actin and β 2-Microglobulin. HIF1 α sized at 181bp, NF κ B sized at 199bp, β -Actin sized at 387bp and β 2-Microglobulin sized at 250bp.

Name	Primer	Product size (bp)	Length	Tm °C	%GC	Acc.No
HIF1 alpha	F: 5' GTCTGAGGGGACAGGAGGAT-3'	181bp	20	64.5	60	U22431
	R: 5' GAAAGGCAAGTCCAGAGGTG-3'		20	63.8	55	
NF κ B	F: 5'-CAGCCCCAGAAACAGCTGAT-3'	199bp	20	53.8	55	X61498
	R: 5'-ACCAGGTCCACCTCGATCTT-3'		20		55	
Beta-Actin	F: 5'-GACCCTTGCCCTCACTGCTTT-3'	387bp	21	68.6	57.1	NG008793
	R: 5'-TTCAGGGGGACCTTGGTCAAT-3'		21		52.4	
Beta 2-Microglobulin	F: 5'-GGCTATCCAGCGTACTCCAAA	250bp	21	71	52	NM004048
	R: 5'-CGGCAGGCATACTCATCTTTTT-3'		22	69	45	

Chapter 3.

Results

3.1 Bioinformatics output

3.1.1 Detection of SNPs and identification of the NFκB1 region

The bioinformatics output showed that the genomic DNA encoding the NFκB p105 subunit is located on chromosome 4 (Figure 7). The protein has 968 amino acids and is 105356 Da in size.

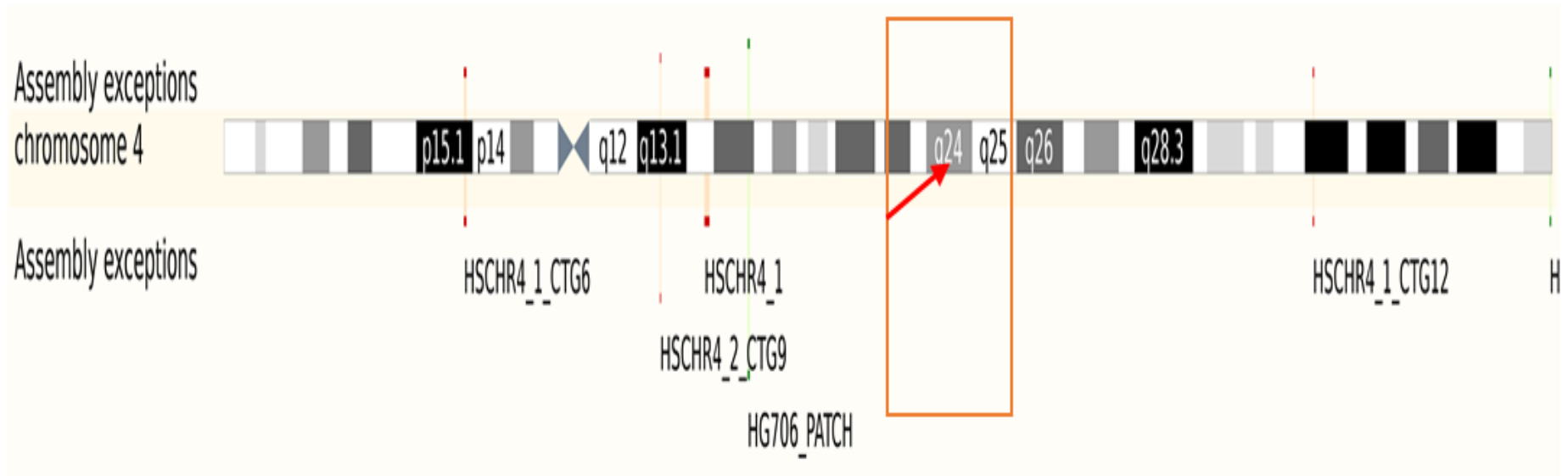


Figure 7: Chromosome 4: 102,939,992-102,951,588, (Ensemble, 2013) and the position of NFκB1 p105 located on chromosome 4. Red box and arrow show NFκB1 gene located on the q arm of chromosome 4 at position 24.

The NCBI programs were used to identify the region of interest and viewed under '*Gene view*'. The '*in gene region*' showed the view of the exonic, intronic and untranslated regions near the SNPs, whilst under the '*gene section*', the graphics view produced the mapping of the SNPs (Table 6).

It was found that there are different classes of variant that may occur in the sequence. These variants can make a change and may have a consequence to the gene product and / or gene expression. Table 6 describes the types of variant identified within the NFκB gene. Consequently, changes may occur in chromosome structure or in a single base in the genetic sequence. Sometimes, these variations might not affect or be linked with a disease because the changes do not influence gene instruction and protein function. Changes in a single nucleotide can lead to disease. Changes in DNA nucleotide may affect protein function. This change may influence gene expression level, and may lead to changes in the biological process through changing RNA and protein regulation.

Table 6: Summary of NFκB1 variants (SNPs) identified in NFκB using Ensemble, 2013

Number of variant consequences	Type of variant	Description of variant
85	Splice region variant	A sequence variant in which a change has occurred within the region of the splice site, either within 1-3 bases of the exon or 3-8 bases of the intron.
88	Non coding exon variant	A sequence variant that changes non-coding exon sequence.
3	Splice donor variant	A splice variant that changes the 2 base regions at the 5' end of an intron.
19	Splice acceptor variant	A splice variant that changes the 2 base regions at the 3' end of an intron.
10306	Intron variant	A transcript: variant occurring within an intron.

Different types of variants were found in NFκB1 (Table 6). Ensemble was then used to identify the NFκB1 sequence variants that are linked with disease. Table 7 shows that there are different variations associated with several different diseases.

Table 7: Variations of NFκB1 in Humans associated with disease

Variation ID	Description	Phenotype(s)
rs230489	A dbSNP ^a Variation	Kidney function and endocrine traits-GFR ^b
rs230529	A dbSNP Variation	Schizophrenia (treatment refractory)
rs230539	A dbSNP Variation	Type II Diabetes Mellitus
rs7665090	A dbSNP Variation	Primary biliary cirrhosis
rs2991716	A dbSNP Variation	Kidney function and endocrine traits-CysC ^c

^adbSNP: The Single Nucleotide Polymorphism Database. ^bGFR: Glomerular filtration rate. ^cCysC: ^cCystatin-C.

As detailed in Table 7, there are many different variants that are associated with many diseases such as, schizophrenia, primary biliary cirrhosis and T2DM. The rs230539 SNP was selected and it is located on Chromosome 4:103495532. This variant has been shown to be associated with T2DM (Ensemble, 2013). This means that there may be a relationship between T2DM and the polymorphisms of NFκB1. This SNP rs230539 (A/G) is located within the intronic region of NFκB1 and this is shown in more detail in Table 8.

Table 8: Details of variant rs230539

Functional class	Wild type nucleotide	Variant nucleotide	Chromosome strand orientation	Chromosome variant position
Intron	A	G	Forward	103714569

The SNPs which mean a variation of the DNA sequence that happen in the genome when a single nucleotide – A, T, C or G (Ensemble, 2013). Table 8 shows the variant of interest is rs230539 SNP, which is intronic variant. Rs230539 A/G genotype in the intron region of NFκB1. In addition, if the R is A it is a wild type nucleotide and if it is G it is a variant nucleotide.

3.1.2 Impact of SNPs

3.1.2.1 Identification of the phosphorylation site

Identification of phosphorylation sites was conducted to find the phosphorylation site and also to determine if the variant was phosphorylated or not.

NetPhos 2.0 was used to identify the phosphorylation sites, if any and the output are shown in Figure 8.

Figure 8 A shows the nucleotide sequence for the region of interest.

DNA is transcribed to RNA, during transcription, introns removed and spliced out by spliceosomes leaving the exons to create the amino acid product *via* translation process. Sometimes, introns are not spliced out during transcription, resulting the intron retained within mRNA as a part of an exon. Phosphorylation has an important role in eukaryotic cells such as gene expression. Some residues are not phosphorylated whether due to the residue not being Serine (S), Threonine (T), or Tyrosine (Y) and they are labelled as a dot or because the score is under the threshold. 'S', 'T', or 'Y' these are being marked if the scores that are over the threshold of 0.500, blue line (Figure 9 C) (Blom *et al.*, 2013). The phosphorylation site in Tyr is one and 40 Thr phosphorylated sites programme predicts, Figure 8B (Blom *et al.*, 2013).

The calculation was preceded by providing a score and a qualitative prediction (probably damaging, possibly damaging, or unknown). The data that is shown in the SIFT column is as a score of the qualitative prediction. For example, if the amino acid change with a score 0 is known as tolerated and mean the protein function is neutral, while the change of amino acid with a score < 0.05 are known as deleterious, which means harmful mutation and can affect protein function and cause disease. In the last column is a PolyPhen-2, which shows the impact of an amino acid change on the function and structure of protein via databases and tools such as the Define Secondary Structure of Proteins tool (DSSP). A prediction for each amino acid change with SIFT tool is calculated. Both score and qualitative prediction (one of 'probably damaging', 'possibly damaging', 'benign' or 'unknown') are provided. Table 9 describes each score (Ensemble, 2013).

Table 9: Score and Qualitative Prediction, (Ensemble, 2013)

Tool	Score	Qualitative prediction
PolyPhen	0	Probably damaging
PolyPhen	1	Possibly damaging
PolyPhen	2	Benign
PolyPhen	3	Unknown
SIFT	0	Tolerated
SIFT	1	Deleterious

According to the results in Figure 8, SNP rs230539 is not phosphorylated. Therefore, PCR approach was selected to investigate rs230539 further.

3.1.2.2 Primer design for PCR

In order to investigate the SNP rs230539, primers were designed for PCR. The FASTA sequence for the region of interest where rs230539 from Ensembl website is located is shown in Figure 9 and the variant location is shown in red with the neighbouring (other) variants shown in blue. Primers have to be designed within the length 18-30 oligo nucleotides to allow a space for restriction enzyme cleavage.

TGTACTTGTGTACAAATTCTGTCTTCTGGATCTATTTTTGTTTAGTTTTTGCCTAATTA
 TGAATTATATTTTTCTATTTCTTTCCATGCCTGTTAGTTTTTTATTGGATGACAGGTATT
 TTGAATTTTGTATCGTTAAGTCTTGGATTCCTTTTTTTTTTTTTTTTTTTGGATGTGCTTT
 TAAATACGTTTGGAGATTGGGATRAAGTTAAATTTGGGAACAGTTTGATTTTTTTGATTC
 TTTCTAAACTTACTTTTAAGCTTTATCAGAGAGACCAGAGAAACCTTTACTCTAGGGTTA
 ATTTGACATCATTGCTAAGGCAGTACCTTTCTGAATTTTCAACCTGATGCTCCATGTATT
 ACAAGATTTCTTGAACTATTCCAGCCCCATATGTGTTACARTAATTTTTCTGCCTCCACC
 TCTGTGGTGGTTCTTTTCCCAGCTTTGACATATTTCCCTCACACACAGCACTCAGCTGAAG
 ACTCCAGTGAYCTCTGAGTGTAYCTCTGTTTGCGGTTTCTTCCTTTCCGGTACTCTGCTT
 GTGAGTTTTAGCCTCYTTGGCTTCCCTCAATATTTAACTGTGTCTCSTCAACCTCAGAGA
 TTGCCAGGCTCTGTTGGGGTTCCCTCCTTCCCTGTGCTGCAGCCTGGGACTCTTTAGGCATT
 AAGCCAGAGTAATTACAGGGTTCACCTTATTTATTTCCCTTTTCTTAAAGATTACTGTTC
 TGTGCTGCCTGTTTTCTAGTGTCTAAAAACCATTTCTTCATGTATTTTWGATATTTAAGG
 TTCAAACCAGTCTGTTTTACT

Figure 9: rs230539 Sequence.

The FASTA sequence indicates the position of the variant rs230539 in red. Blue text shows the other variants and the sequences that are underlined are primers.

3.1.3 DNA detection

Amplification of genomic DNA was performed using PCR followed by analysis of the products using agarose gel electrophoresis. PCR amplification was performed with different primer concentrations (0.2, 0.5 or 1 μ M) to find the optimum concentration for this set of experiments (Figure 10).

3.1.3.1 PCR gel electrophoresis

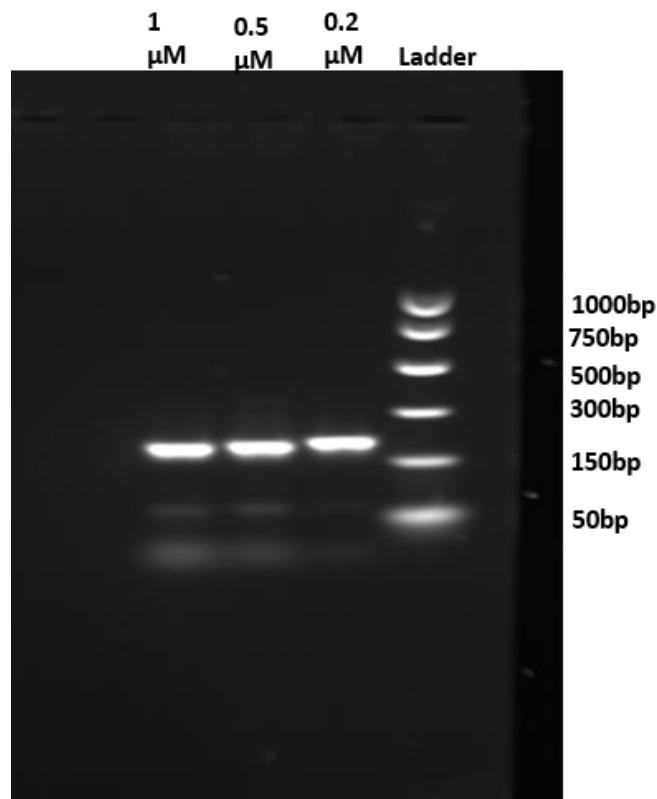


Figure 10: PCR product following amplification with NF κ B primers generated using different primer concentrations 0.2 – 1 μ M

Figure 10 shows that the calculated fragment size of the PCR product was 195 bp, which was predicted to be 206 bp. PCR products were amplified with different primer concentrations: 0.2, 0.5 and 1 μ M in order to choose the best primer concentration for further experiments. A primer concentration of 0.2 μ M was used in all subsequent experiments as it gave the cleanest band at the correct size, with no additional smaller bands as is evident when using 0.5 and 1.0 μ M which show faint or smeared bands (Figure 10).

3.1.3.2 PCR with restriction enzymes

The amplified fragments were cut with an enzyme known to cleave DNA at the SNP site of interest (rs230539). Images of gels showing restricted and unrestricted PCR product using HpyCH4iii with different periods of incubation (A) 1 hour, (B) 4 hours and (C) 24 hours. Figure 11(A, B and C) showed there was no digestion of the fragment.

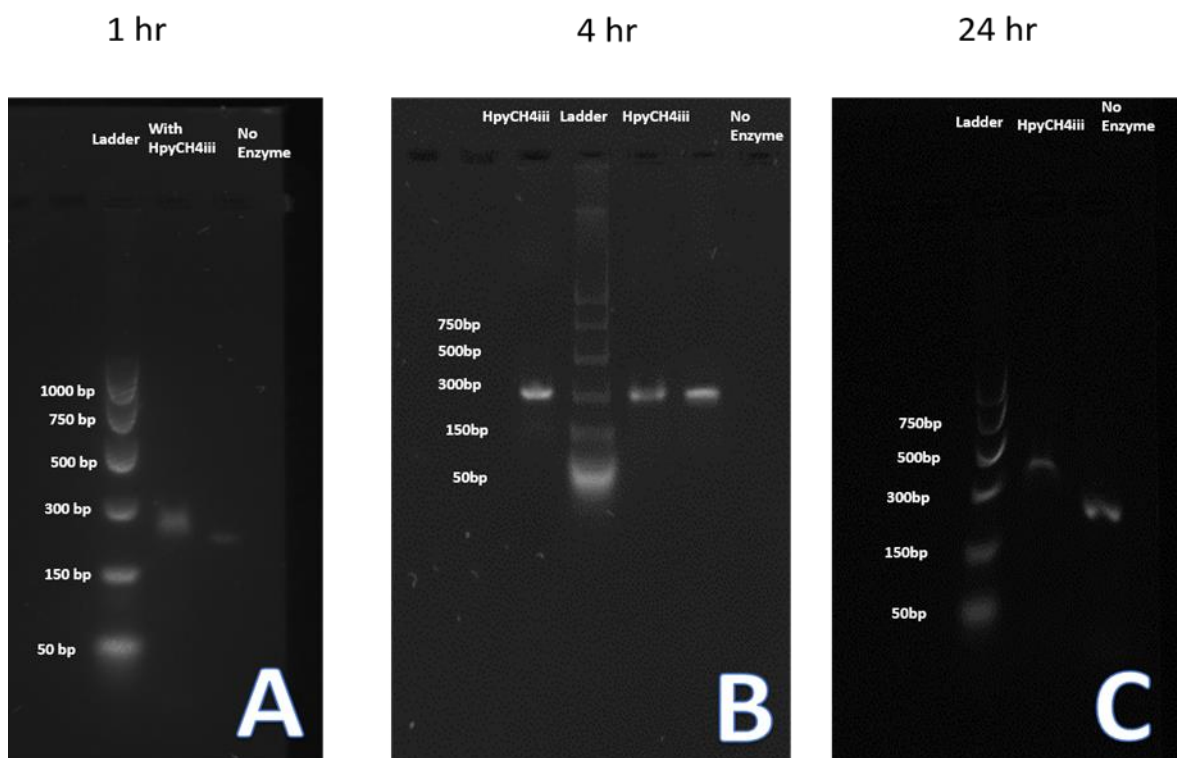


Figure 11: A 1 hr incubation with HpyCH4iii at 37°C, the restriction was carried out for 4 hr at 37°C (B) and 24 hr (C).

The uncut size of the calculated fragment size was 197 bp which was close to the predicted size of 206 bp, whereas the product with HpyCH4iii enzyme increased in size to around 260 bp when incubated for 1 hour (Figure 12A). The gel showed that there was no digestion with this enzyme (HpyCH4iii) after 4 hr incubation at 37°C and that the fragment size increased from 206 bp to 260 bp when the sample was incubated for 1 hour and to 380 bp after 24 h incubation (Figure 11). This might indicate

binding of the enzyme to the substrate (Figure 11A and 11C). Also, Figure 11B showed that the digestion did not work and the calculated fragment size was 197 bp which was predicted to be 206 bp.

Therefore, other restriction enzymes were used: Alu1 and PvuII, and the results are shown in Figure 12.

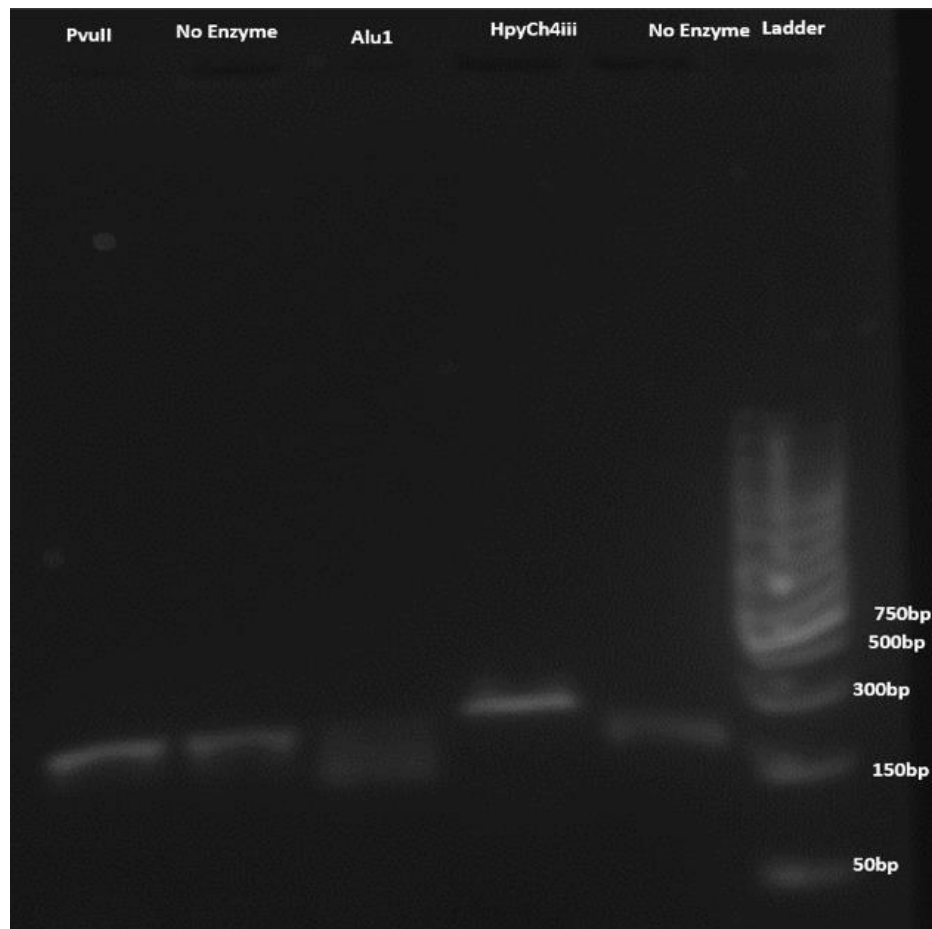


Figure 12: Restriction with HpyCH4iii, Alu1 and PvuII incubated for one hour at 37°C.

The results show that there was no digestion of the product after using enzymes HpyCH4iii (which supports the result shown in Figure 11) and PvuII, whereas it appears that Alu1 has cut the product (Figure 12). NEB cutter predicted the PCR product was digested by two restriction enzymes specific for the region amplified, which are HpyCH4iii and Alu1. There are two bands in the Alu1 lane and their size is 164 bp and 219 bp. Alu1

should cut in one site at AGCT length 175/177bp. According to HpyCh4iii it is larger than 206 bp, and its size is 293 bp.

According to our results from the gel, the fragments were uncut, by HpyCh4iii as shown in Figures 11 and 12. The PCR product when digested with HpyCH4iii increased in size to around 290 bp. However, these restriction enzymes were predicted to digest according to the NEB cutter software except PvuII but *in vitro* it appears that this was not demonstrated in these experiments. To further investigate the sequence, the DNA samples were sent for sequencing.

3.1.4 DNA Sequencing

3.1.4.1 PCR purification and DNA detection

A sample of DNA was purified using the Qiagen MinElute Reaction Cleanup Kit and the size confirmed by resolution in an agarose gel (Figure 13).

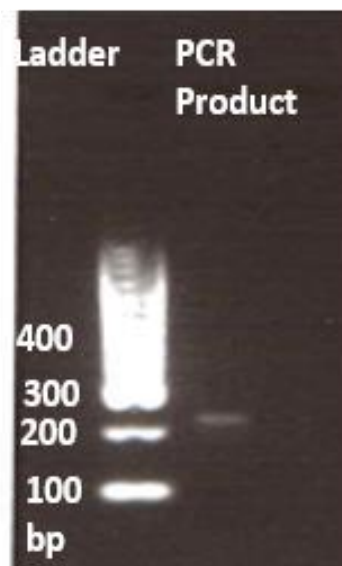


Figure 13: PCR purification of gDNA via gel electrophoresis

Figure 13 shows the fragment size for the PCR product alongside the DNA ladder, after purification, the calculated fragment size was 199 bp which was predicted to be 206 bp and the sequence output is shown in Section 3.1.4.2.

3.1.4.2 Sequence output

DNA sequencing was used because the digestion of the fragment with restriction enzymes was unsuccessful. Therefore, the sample was sent to Dundee University for sequencing and shown below is the sequence output (Figure 14).

Predicted amplified sequence

A
CAGAGAGACCAGAGAAACCTTTACTCTAGGGTTAATTTGACATCATTGCTAAGGCAGTACCTTTCTGAAT
TTCAACCTGATGCTCCATGTATTACAAGATTTCTTGAAGTATTCCAGCCCCATATGTGTTACAAATTTT
TCTGCCTCCACCTCTGTGGTGGTTCTTTCCAGCTTTGACATATTTCTCACACACAGCACTC

DNA SEQUENCE obtained from Dundee sequencing labs

B
CGGATGTCATTGCTAGGCAGTACCTTTCTGATTTTACCTGATGCTCCATGTATTAAAGATTCTTGAACTA
TTCCAGCCCCATATGTGTTACAATAATTTTTCTGCCTCCACCTCTGTGGTGGTTCTTTCCCGATCTTACAC
CTGTTTCATCACACACAGCACTATAACGATATTATTGAGGCTCACAGAGAACAGATTGGTGGTATGACAG
TGTTTGCCGGAACACCTCCAACCGTGGATTCCCACTGGAAGTC

Figure 14: (A) Predicted DNA sequence and (B) DNA sequence obtained from Dundee. The highlighted regions show the restriction site for enzymes HpyCH4iii (green) and Alu1 (blue).

GACAT* *CATTGCTAAGGCAGTACCTTTCTGAATTTTCAACCTGATGCTCCATGTATTACAA
 CGGATGTCATTGCTA*GGCAGTACCTTTCTGA*TTTTCA*CCTGATGCTCCATGTATTA*AA
 GATTTCTTGAAC TATTCCAGCCCCATATGTGTTACAR TAATTTTTCTGCCTCCACCTCTGTG
 G*TT*CTTGAAC TATTCCAGCCCCATATGTGTTACAA TAATTTTTCTGCCTCCACCTCTGTG
 GTGGTTCTTTTCCCAGCTTTGACATATTTCCCTCACACACAGCACTC
 GTGGTTCTTTTCCCGATCTT*ACACCTGTT CATCACACACAGCACTA

Figure 15: Sequence Alignment.

The nucleotides in blue show regions where the nucleotide sequence is incorrect and the position of the * shows missing data. The highlighted region shows the sequence of the SNP is A. The nucleotides in red are the published sequence and the lower black text is the amplified sequence output.

The predicted sequence and the sequence obtained for the Dundee sequencing lab were compared and are presented in Figure 15. Sequence alignment was used to compare between the two sequences and to determine their similarity. According to above aligned sequences (predicted sequence in red and obtained sequence from Dundee in black), there is a mismatch (as shown in blue) and a couple of gaps (represented by *) and this may affect the identity. Similarity between two sequences is 94% (i.e. 12 of 206 nucleotide mismatch) when adjustments are made to alignment when incorporating the gaps.

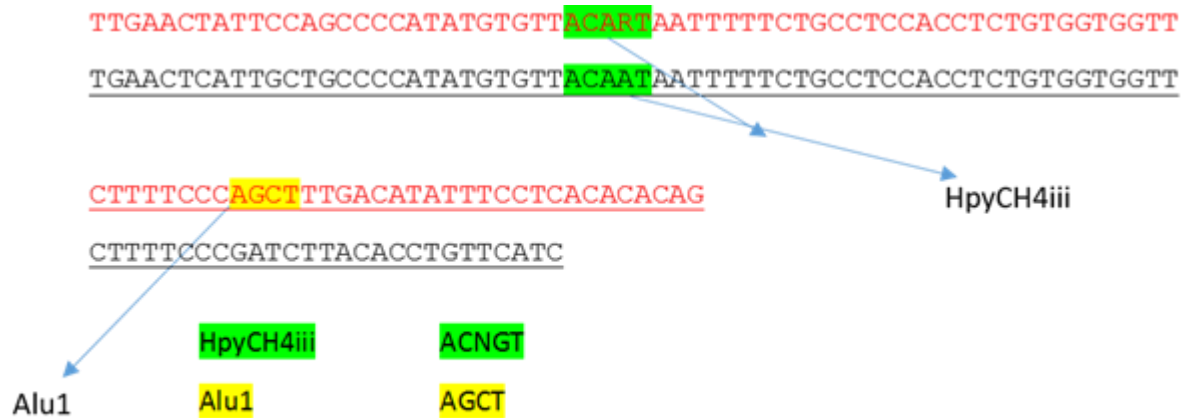


Figure 16: Restriction sites for enzymes HpyCH4iii and Alu1.

The highlighted regions show the restriction site for enzymes HpyCH4iii (green) and Alu1 (blue).

With time constraints it was not possible to follow this up further in this study but work progressed by examining the way that the NFκB and HIF1α genes could be regulated in response to glucose concentration.

3.2 RNA Detection

To investigate the regulation and expression of NFκB1, mRNA level was measured following exposure of U937 cells to high glucose concentrations. cDNA was amplified with 0.2 μM NFκB, 0.2 μM HIF1α and 1 μM β2-microglobulin primers after 24 hours incubation in different glucose conditions (5.5 mM, 20 mM and 40 mM) to determine any changes in the

level of NF κ B, HIF1 α and β 2-microglobulin in response to different glucose concentrations.

RNA was extracted using trizol and purified from U937 cells (See Figure 17).

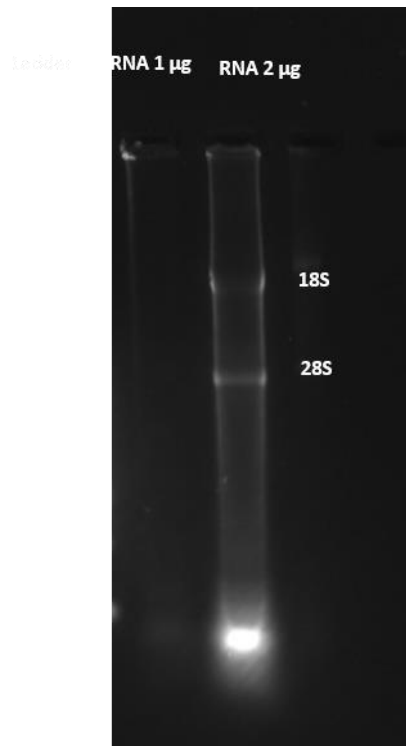


Figure 17: RNA gel electrophoresis of RNA bands using trizol (ratio: 2.4)

Figure 17 details that the RNA bands (18S and 28S) were observed in Lane 2: 2 μ g RNA loaded to well, whereas in Lane 1: 1 μ g RNA was loaded and their RNA bands (18S and 28S) are not clear. This could be due to there not being enough RNA loaded in Lane 1 as only 1 μ g RNA was used. Whereas in Lane 2, 2 μ g RNA was used and the two faint bands for RNA, which are 28S and 18S ribosomal RNAs, were visible. Also RNA was degraded as evident with the band identified.

cDNA samples were prepared from each of the RNA samples from U937 cells treated as specified in the text (Section 2.4) and amplified with β -Actin primers (Table 6) (in Figure 18) to check the level of the respective mRNA.

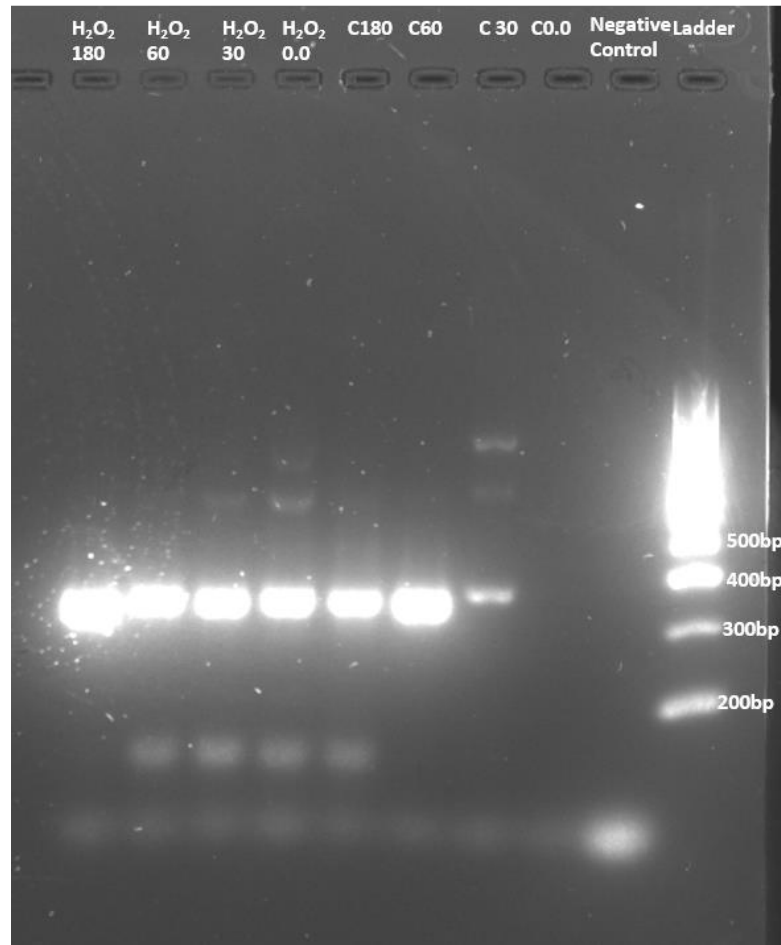


Figure 18: Gel electrophoresis for cDNA amplification with 0.5 μ M β -Actin primers following different incubation times, with and without H₂O₂, (C is for a control).

Figure 18 shows the gel electrophoresis for cDNA amplification with β -Actin following different incubation times of 0, 30, 60 and 180 minutes, with and without H₂O₂ (10 μ M). There is a clear band observed and it was calculated to be 381 bp in size which was predicted to be 387 bp with control condition (denoted by C) during incubation times of 30, 60 and 180

minutes. In addition, there was also a band detected after incubation in the presence of H₂O₂ for 0, 30, 60 and 180 minutes.

cDNA amplification with 0.5 μM β-Actin was repeated on the following day with different set of cDNA samples and results are shown in Figure 19.

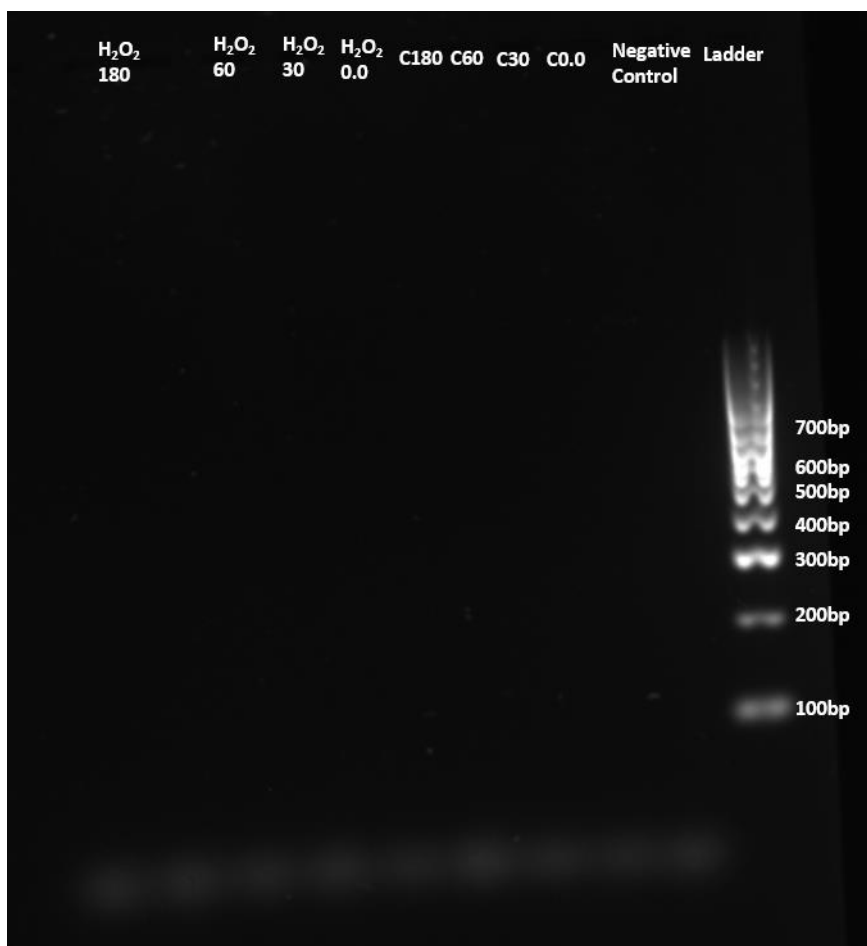


Figure 19: Gel electrophoresis for cDNA amplification with 0.5μM β-Actin primers with different incubation times with and without H₂O₂.

Figure 19 shows the gel electrophoresis for cDNA amplification with 0.5 μM β-Actin with 0 30, 60 and 180 minutes incubation with and without H₂O₂. After repeating this experiment several times with 0.5 μM β-Actin, it did not work in the same way as Figure 18, as shown in Figure 19 and there was no evidence of amplification.

3.2.2 cDNA amplification with HIF1 α and NF κ B primers

U937 cell cDNA was amplified with HIF1 α primer with/without the Taq in order to check that there was not any contamination and to confirm the fragment size (Figure 20).

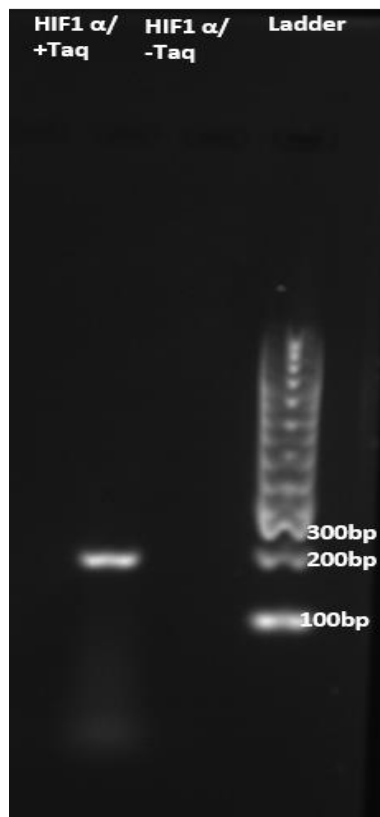


Figure 20: Gel electrophoresis for PCR samples with HIF 1 α primers

Figure 20 shows gel electrophoresis for cDNA amplification with HIF1 α . First lane (From right to left) was the ladder, lane 2 was HIF1 α with no Taq, and lane 3 was HIF1 α with Taq. HIF1 α with Taq shows a clear band

with size around 181 bp, which was at the correct size predicted from sequence information.

cDNA amplification with NFκB primers was then carried out to check the band size of this product.

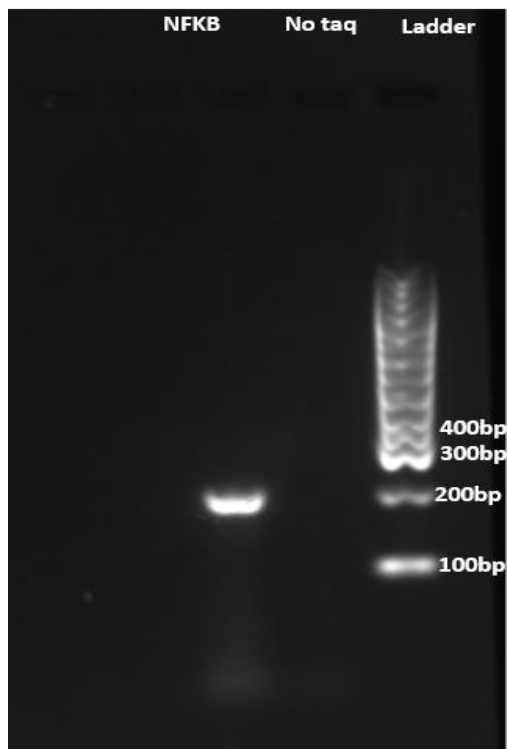


Figure 21: Gel electrophoresis cDNA amplification with NFκB primers

Figure 21 shows cDNA amplification with NFκB primer and there was band sized at 199 bp. Then, the test samples were then amplified with NFκB and HIF1α with and without H₂O₂ at same concentrations as before.

3.2.3 cDNA amplification with NFκB and HIF1 α primers (Control (C) and H₂O₂)

RNA extraction was followed by cDNA was amplified with NFκB and HIF1 α.

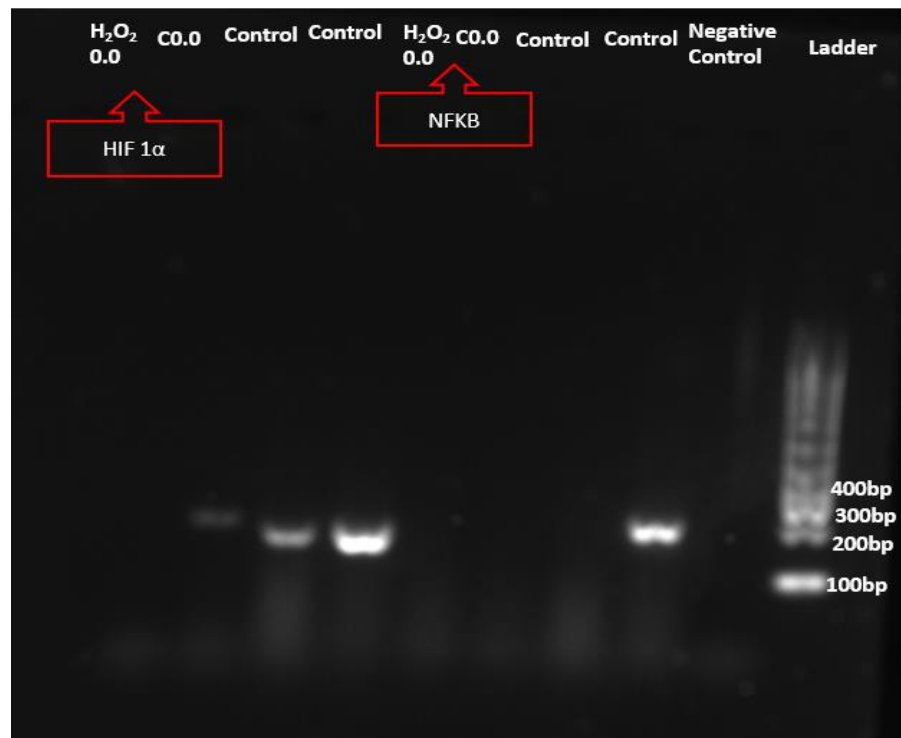


Figure 22: Gel electrophoresis cDNA amplification with NFκB and HIF1α primers

Figure 22 shows the gel electrophoresis for cDNA amplification with NFκB and HIF1α, with and without H₂O₂ after 0 minutes. Lane 1 (From right to left): ladder, Lane 2: negative control, Lane 3: Control (cDNA used previously, Figure 21), Lane 4: Control (fresh cDNA), Lane 5: C0.0 min with NFκB, Lane 6: H₂O₂ with NFκB, Lane 7: Control (cDNA used previously, Figure 20), Lane 8: Control (fresh cDNA), Lane 9: C0.0 min with HIF1α and Lane 10: H₂O₂ with HIF1α. This experiment worked for HIF1α as a band with HIF1α was evident at 181 bp for control (0 minutes). However, this was not the case with NFκB as no bands were observed with

any of the conditions tested. The (Control) was cDNA sample from 10 million cells that was prepared previously. Also, cDNA sample from 10 million cells that freshly made.

To repeat the experiment shown in Figure 22, cDNA amplification with HIF1 α was conducted to check the gene expression during different incubation times with and without H₂O₂.

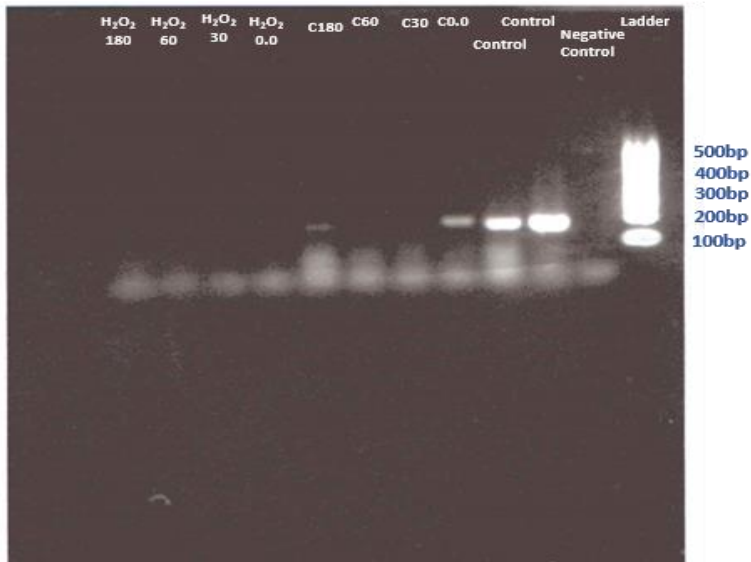
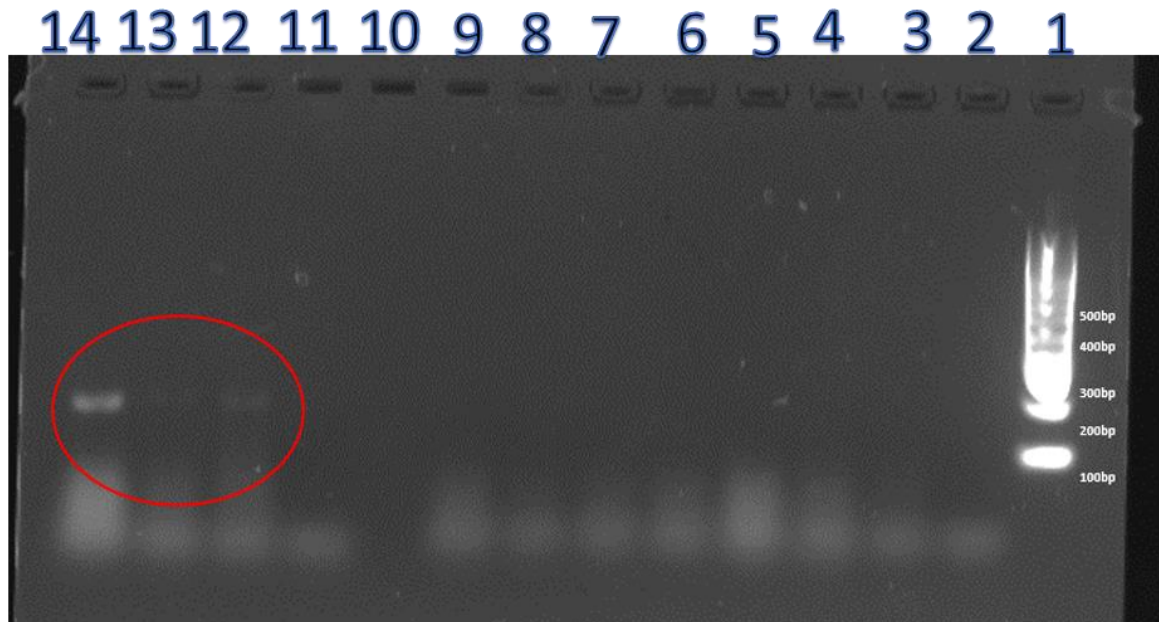


Figure 23: Gel electrophoresis for cDNA amplification with HIF1 α primers with different incubation times with and without H₂O₂

Figure 23 shows the gel electrophoresis result for cDNA amplification with 0.2 μ M HIF1 α during different incubation times: 0 minute, 30 minutes, 60 minutes and 180 minutes with and without H₂O₂ (10 μ M). The expression of HIF1 α was evident with incubation times of 0 and 180 minutes without H₂O₂ (181 bp).

As the cDNA amplification with β -Actin primers did not work (Figure 19), amplification with β 2-microglobulin primers was carried out as it is another type of housekeeping gene.

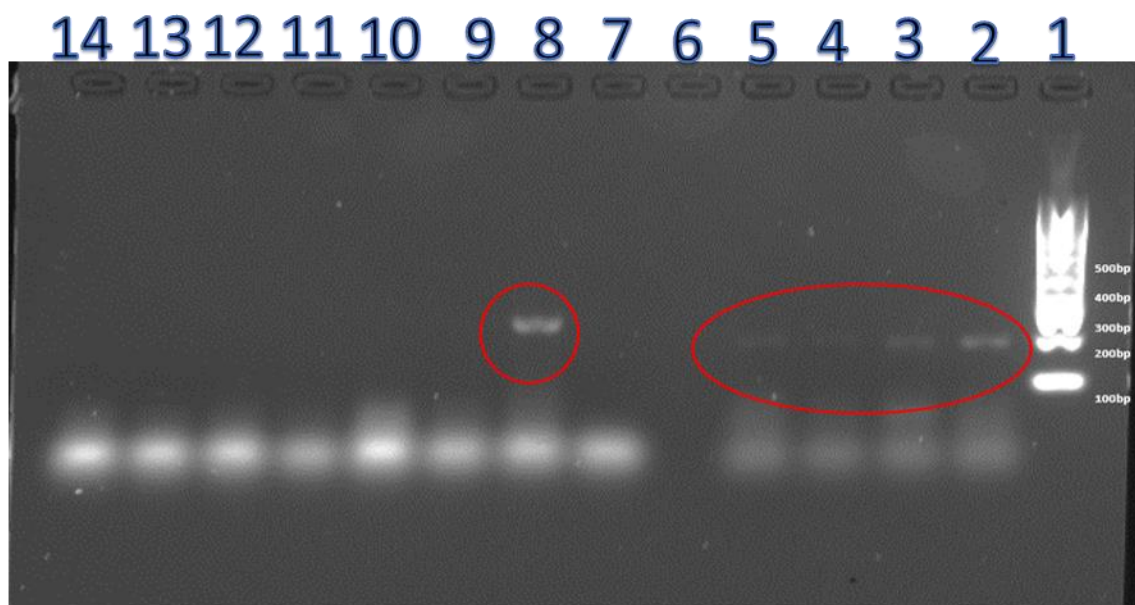
3.2.4. cDNA amplification with NFkB, HIF1 α and β 2-microglobulin primers with different glucose concentrations



Lane Number	Sample
1	Ladder
2	Negative Control {NFkB}
3	Time 0.0 {NFkB}
4	5.5 mM (1) {NFkB}
5	5.5 mM (2) {NFkB}
6	20 mM (1) {NFkB}
7	20 mM (2) {NFkB}
8	40 mM (1) {NFkB}
9	40 mM (2) {NFkB}
10	Space
11	Negative Control {HIF1 α }
12	Time 0.0 { HIF1 α }
13	5.5 mM (1) { HIF1 α }
14	5.5 mM (2) { HIF1 α }

Figure 24: Gel electrophoresis for cDNA amplification with 0.2 μ M NFkB and HIF1 α primers in different glucose concentrations. NFkB was not expressed in this cell. HIF1 α in lanes 12, 13 and 14 was expressed with size 181 bp. The table shows the lane number and the samples.

cDNA amplification with HIF1 α and β 2-microglobulin primers with different glucose concentrations is shown below in Figure 25.



Lane Number	Sample
1	Ladder
2	20 mM (1) { HIF1 α }
3	20 mM (2) { HIF1 α }
4	40 mM (1) { HIF1 α }
5	40 mM (2) { HIF1 α }
6	Space
7	Negative Control { β 2- microglobulin}
8	Time 0.0 { β 2- microglobulin}
9	5.5 mM (1) { β 2- microglobulin}
10	5.5 mM (2) { β 2- microglobulin}
11	20 mM (1) { β 2- microglobulin}
12	20 mM (2) { β 2- microglobulin}
13	40 mM (1) { β 2- microglobulin}
14	40 mM (2) { β 2- microglobulin}

Figure 25: Gel electrophoresis for cDNA amplification with 0.2 μ M HIF1 α and β 2-microglobulin primers in different glucose concentrations. HIF1 α was expressed and shown in lanes 2, 3, 4 and 5. Lane 8 shows the expression of β 2-microglobulin.

Figures 24 and 25 show images of electrophoresis gels for cDNA amplification with NF κ B, HIF1 α and β 2-microglobulin in different glucose concentrations, which were 5.5, 20 and 40 mM. NF κ B was not shown to be expressed in this cell line, whereas bands for HIF1 α expression were identified and calculated to be 181 bp in size, which is the correct size. In addition, there was a clear band for β 2-microglobulin with normal glucose condition (5.5 mM) and the calculated band size was 251 bp, which aligned with the predicted size but this was not seen in the other experimental conditions.

Chapter 4: Discussion

4.1 SNP detection

To identify the genetic variations in the NFκB1 gene that are associated with diabetes, the NFκB1 gene was examined and one SNP was selected within the NFκB gene that has been identified and associated with diabetes (Ensemble, 2013). This was rs230539. According to the genotype data from Ensemble website, rs230539 is an intronic variant and located in chromosome 4 at 4q24 in position 103495532. Rs230539 (G/A) where this polymorphism was reported to be associated with type 2 diabetes (Kent *et al.*, 2014). There are different reports illustrating that genetic variation in the intron region are involved in changes to transcript processing (Kent *et al.*, 2014). Through a splicing step, introns need to be taken off from the pre-mRNA. Intronic SNPs may have an effect on gene expression and also may affect transcriptional regulation. Transcriptional regulation is a process that can adjust the transformation of DNA to RNA. As a result of that, it regulates the activity of the gene (Lewin 2004).

NFκB1 polymorphism was determined by using restriction fragment length polymorphism (RFLP) with different restriction enzymes. Initially the HpyCH4iii restriction enzyme was used (incubated for 60 minutes), but the enzyme did not digest the PCR product and the size of the band increased to 260 bp from 206 bp and there was no obvious reason for this.

Therefore, the experimental conditions were changed to 4 hours and 24 hours incubations. The fragment size when incubated for 4 hours was 217 bp which is consistent with what was expected, whereas with an overnight incubation, the fragment size increased to 359 bp. This may be due to binding of DNA to the enzyme according to the manual from New England Biolabs (New-England-Biolabs-Inc. 2010). As larger bands are shown in the gel after digestion, this may be due to binding of enzyme to the substrate. Also, over digestion of more than 4 hours is not recommended and may cause changes in the fragment size (New-England-Biolabs-Inc. 2010). However, this does not explain the result found after 1 hour

restriction. This increased size may result from alteration of band size due to dimer formation. During the last step of PCR, which is cooling step, hybridisations may occur (New-England-Biolabs-Inc. 2010).

Another two enzymes, Alu 1 and PvuII were used (one-hour incubation according to manufacture's protocol) and run alongside the HpyCH4iii enzyme on the same gel. According to the results for PvuII there was no cleavage of the DNA, this is consistent with predicted sequence information. The PCR product appeared to have been partially digested with Alu1. There are two bands in the Alu1 lane and their size was recorded as 164 bp and 219 bp. Alu1 should cut in one site at AGCT length 175/177 bp. This may be due to restriction enzyme digestion not fully digesting the DNA and therefore evidence of uncut and cut DNA remains. This could be due to the incubation time not being long enough or too few units of the enzyme used. After sequencing the PCR product, results show the similarity between two sequences is around 94%. According to sequencing result, HpyCH4iii enzyme did not cut because of the wild type (A) is present. Alu1 did not cut because it will be heterozygous, which means one of the DNA strand has restriction site, which is one with right sequence and one does not due to change in the sequence. This means that two sequences have the same length, similar gene sequences and have similar structures. As no one has examined the gene databases to identify the SNP rs230539 in NFκB before in U937 cells, therefore, this finding is novel and an interesting finding in this study.

4.2 Standardisation of NFκB, RT-PCR and the effect of different glucose concentrations

Initially, 1×10^4 U937 cells/ml was used in 6 well plates, which was found to be not a sufficient number of cells, and may explain why the RNA concentrations were initially so low. Therefore, number of U937 cells was optimised to provide a sufficient RNA concentration and quality. After

using 1×10^7 U937 cells and RNA extracted using Trizol reagent. The RNA concentration was high ($2.4 \mu\text{g}/\mu\text{l}$). In addition, the RNA concentrations were high, but bands were not clear and RNA quality was low. This may be due to only $1 \mu\text{g}$ of the sample being added and this was not enough. In the other lane, $2 \mu\text{g}$ was used and the two bands for RNA, which are 28S and 18S ribosomal RNAs, were visible. However, it seems that the RNA had degraded partially, which is evident by the smeared appearance and lack of sharp bands. (Thermo Fisher 2015) .

RT-PCR was used for the amplification of cDNA with β -Actin, HIF1- α , β 2-microglobulin and NF κ B. β -Actin worked the first time the experiment was conducted but, when it was repeated, it did not work and this may be due to storage of RNA that may affect the RNA quality and/or it may have degraded due to inherent enzyme contamination. Moreover, the amplification of cDNA with HIF1- α at the start of the experiment (0 minute) without H_2O_2 worked with a band observed at 181 bp, whereas no band was observed when incubated with H_2O_2 0 minute. This may indicate that the number of surviving cells was low or that H_2O_2 may cause cellular dysfunction and the cells to die (Coyle *et al.* 2006) even after the very short exposure.

Furthermore, the NF κ B PCR product was not detected during different incubations with various glucose concentrations, whereas, HIF1 α expression appeared to decrease during high glucose concentrations (40mM). The NF κ B PCR product was not detected, this may lead to incubation times not being long enough and that longer than 24 hours should be investigated. In other research with U937 (Guha *et al.* 2000), the regulation of TNF α and NF κ B *via* exposure of the cells to chronic high glucose concentrations is reported after 2 days incubation in the absence of further stimulation. These observations will need to be verified by repeating these experiments. It appears that there is perhaps something about these cells that do not lend themselves to this experimental approach. This may be due to the fact that U937 cells are a suspension cell line and are generally used following stimulation with LPS (*E. coli* Lipopolysaccharide) (Baek *et al.*, 2009). In addition, U937 can first differentiate into macrophage by incubation with 10 ng/ml of PMA (phorbol

12-myristate 13-acetate) for 24 hours and also can be activated with 1µg/ml of LPS (E-coli lipopolysaccharide) for 6 hours to copy inflammatory response of stimulated macrophages (Ghosh *et al.* 2010).

There is a study shows that, culturing U937 cells treated with LPS in medium containing high glucose for 2 weeks or longer caused an important increase in gene expression and caused stimulation of Matrix metalloproteinase-1 (MMP-1) and mononuclear cells of tumor necrosis factor-α (TNFα). LPS and high glucose increase CD14 in U937 cells by prompting the transcription activity of NFκB and AP-1 (Nareika *et al.* 2008). In this research, monocyte was used as it is circulate in blood before entering tissue and expresses different cytokines. Several studies with Thp1 show that high glucose stimulates monocytes and encourage the TNF-α activation via NFκB (Shanmugam *et al.* 2003). U937 cells have been used in several studies to investigate different biological approaches linked to monocyte and macrophage function such as monocytic differentiation (Baek *et al.*, 2009).

4.3 Conclusion

The essential conclusions from this work to date are:

1. RFLP and sequencing demonstrated that U937 cells express the wild type form of rs230539.
2. Restriction digestion with HpyCH4iii was problematic if 4 hour incubation is not used.
3. U937 cells have the potential for use as a model for determining the effect of glucose concentration on gene expression but the following must be considered with further studies:
 - a. The role of stimulation of the cells
 - b. The repeatability of the observed changes in expression of NFκB and HIF1α
 - c. The effect of duration of exposure to the test conditions on the results.

4.4 Future Work

If time allowed there are a number of ways this work could be extended. For example, U937 cells could be cultured under different glucose concentrations and incubated for more than 24 hours to determine the role of NFκB activation. U937 cells could be treated with phorbol 12-myristate 13-acetate (PMA) for 12 to 24 hours to activate monocytic differentiation.

Another example U937 cells could be cultured under hypoxia (<5%) in a range of glucose concentrations to address the biological significance of NFκB activation. Afterwards, the supernatants would be analysed for the protein level expression using ELISA. The cells would be incubated alone (control cells) and /or incubated with H₂O₂ to show the response to the oxidative stress and to demonstrate the effect of oxygen on inflammatory

mediators responsible for the vascular complications in diabetes (Nareika *et al.* 2008). Western blot could be used to test for an increase in NFκB proteins, but also to determine the protein expression of inflammatory cytokines with high glucose concentrations and measure the changes in nuclear NFκB after incubation in high glucose concentrations.

References

- Ahmad, S., 2013. *Diabetes: An Old Disease, a New Insight*, Springer Science & Business Media
- Aiello, LP., 2002, The potential role of PKC in diabetic retinopathy and macular edema, *Survey of Ophthalmology*, 47(2), pp. S263-S269.
- Alghadyan, AA., 2011, Diabetic retinopathy – An update, *Saudi Journal of Ophthalmology*, 25(2), pp. 99-111.
- Allman, T., 2008. *Diabetes*, Infobase Publishing.
- Andreasen, A. Meghan, K. Ronan, M. Kirsten, M. and Bente, K., 2011. Type 2 diabetes is associated with altered NF- κ B DNA binding activity, JNK phosphorylation, and AMPK phosphorylation in skeletal muscle after LPS. *PLoS one*, 6(9), p.e23999.
- Atkinson, M., 2012. The pathogenesis and natural history of type 1 diabetes. *Cold Spring Harbor perspectives in medicine*, 2(11), pp.1–18.
- Aveleira, C., 2009, The role of inflammatory mediators in retinal microvascular dysfunction: implications for the blood-retinal barrier breakdown in diabetic retinopathy. University of Coimbra, Coimbra, pp.9–181.
- Baek, Y. Haas, S. Hackstein, B. Holger, G. Hernandez, Santana, M. Lehrach, H. Sauer, S & Seitz, H., 2009. Identification of novel transcriptional regulators involved in macrophage differentiation and activation in U937 cells, *BMC Immunology*, 10:18, pp. 1-15.
- Balasubramanyam, M, Rema, M & Premanand, C., 2002, Biochemical and molecular mechanisms of diabetic retinopathy, *Current Science*, 83(12), pp. 1506-1514.
- Bergers, G. Song, S., 2005. The role of pericytes in blood-vessel formation and maintenance. *Neuro-Oncology*, 7(4), 452–464.
- Blom, N., Gammeltoft, S., and Brunak, S., 2013. Sequence- and structure-based prediction of eukaryotic protein phosphorylation sites., *NetPhos 2.0 server*. [online] *Journal of Molecular Biology*. Available from: <http://www.cbs.dtu.dk/services/NetPhos/> [Accessed september 2013].
- Brownlee, M., 2001, *Biochemistry and molecular cell biology of diabetic complications*, *Nature*, 414(6865), pp. 813-820.
- Brownlee, M., 2005, The pathobiology of diabetic complications: A unifying mechanism, *Diabetes*, 54(6), pp. 1615-1625.
- Cade, W.T., 2008. Diabetes-related microvascular and macrovascular diseases in the physical therapy setting. *Physical therapy*, 88(11), pp.1322–1335.

- Catrina, S. Kensaku, O. Teresa, P. Kerstin, B. & Lorenz, P., 2004. Hyperglycemia Regulates Hypoxia-Inducible Factor-1 α - Protein Stability and Function, *Diabetes* 53(12), pp.3226–32.
- Chakrabarti, S., 2007, *Diabetic retinopathy: From pathogenesis to treatment*, Hindawi Publishing Corporation, New York, NY.
- Chen F., 2014. NFKB1 (nuclear factor of kappa light polypeptide gene enhancer in B-cells 1). [online] Atlas of Genetics and Cytogenetics in Oncology and Haematology. Available from: <http://atlasgeneticsoncology.org/Genes/NFKB1ID323.html> [Accessed September 2013].
- Chen, S, Xue, Y, Zhang, X, Wu, Y, Pan, J, Wang, Y & Cheng, J., 2005, A new human acute monocytic leukaemia cell line SHI-1 with t(6;11) (q27;q23), p53 gene alterations and high tumorigenicity in nude mice, *Haematologica*, 90(6), pp. 766-775.
- Chistiakov, DA., 2011, 'Diabetic retinopathy: Pathogenic mechanisms and current treatments', *Diabetes & Metabolic Syndrome*, 5(3), pp. 165-172.
- Coyle, C. H., Martinez, L. J., Coleman, M. C., Spitz, D. R., Weintraub, N. L., & Kader, K. N., 2006. Mechanisms of H₂O₂-induced oxidative stress in endothelial cells. *Free radical biology & medicine*, 40(12), pp.2206–2213.
- Detrick, B., & Hooks, J. J., 2010. Immune regulation in the retina. *Immunologic Research*, 47(1-3), 153–161.
- Diabetes UK, 2010. Key statistics on diabetes. *Diabetes*, 692(March), pp.1–21.
- Di Iorgi, N., Napoli, F., Allegri, A. E. M., Olivieri, I., Bertelli, E., Gallizia, A., Maghnie, M., 2012. Diabetes Insipidus; Diagnosis and Management. *Hormone Research in Paediatrics*, 77(2), pp.69–84.
- Donnelly, R., Idris, I., & Forrester, J. V., 2004. Protein kinase C inhibition and diabetic retinopathy: a shot in the dark at translational research. *The British Journal of Ophthalmology*, 88, pp. 145-151.
- Duh, E. & Aiello, L.P., 1998 *Perspectives in Diabetes*. , pp.1899–1906.
- Ensembl. 2013. [online] Wellcome Trust Sanger Institute. Available from: http://www.ensembl.org/Homo_sapiens/Search/Results?species=Homo_sapiens;idx=;q=NFKB1 [Accessed February 2013 2013].
- Faideau, B., Larger, E., Lepault, F., Carel, J. C., & Boitard, C., 2005. Role of beta-cells in type 1 diabetes pathogenesis. *Diabetes*, 54, pp.s87–s96.
- Fhearraigh, S., Signalling pathways involving Protein kinase C (PKC) | Abcam. Available at: <http://www.abcam.com/cancer/signaling-pathways-involving-pkc> [Accessed November 3, 2015].
- Fowler, MJ 2008, 'Microvascular and macrovascular complications of diabetes, *Clinical Diabetes*, 26(2), pp. 77-82.

Gao, W., Ferguson, G., Connell, P., Walshe, T., Murphy, R., Birney, Y. A., Cahill, P. A., 2007. High glucose concentrations alter hypoxia-induced control of vascular smooth muscle cell growth via a HIF-1 α -dependent pathway. *Journal of molecular and cellular cardiology*, 42(3), pp.609–19.

Gene cards. 2013. [online] Weizmann Institute of Science. Available from: <http://www.genecards.org/cgi-bin/carddisp.pl?gene=NFKB1&search=NFKB1> [Accessed February 2013 2013].

Ghosh, C. C., Ramaswami, S., Juvekar, A., Vu, H.-Y., Galdieri, L., Davidson, D., & Vancurova, I., 2010. Gene-specific repression of proinflammatory cytokines in stimulated human macrophages by nuclear I κ B α . *Journal of immunology (Baltimore, Md.: 1950)*, 185(6), pp.3685–93.

Guha, M., Bai, W., Nadler, J. L., & Natarajan, R., 2000. Molecular Mechanisms of Tumor Necrosis Factor Gene Expression in Monocytic Cells via Hyperglycemia-induced Oxidant Stress-dependent and -independent Pathways. *Journal of Biological Chemistry*, 275(23), 17728–17739.

Hammes, H.-P., Feng, Y., Pfister, F., & Brownlee, M., 2011. Diabetic Retinopathy: Targeting Vasoregression. *Diabetes*, 60(1), pp.9–16.

Kerry, A., 2013. Retina. [online] Assil Eye Institute. Available from: <http://www.assileye.com/los-angeles/diabetic-retinopathy.htm> [Accessed 15/4/2013 2013].

King, GL 2008, The role of inflammatory cytokines in diabetes and its complications, *Journal of Periodontology*, 79(8), pp. 1527-1534.

Kowluru, RA, Zhong, Q & Kanwar, M., 2010, Metabolic memory and diabetic inflammatory mediators in retinal pericytes, *Experimental Eye Research*, 90(5), pp. 617-623.

Lang, G., 2007, Treatment of diabetic retinopathy with protein kinase C subtype beta, In W. Behrens-Baumann (eds), *Diabetic retinopathy*, Kanger, Geneva, pp. 11-32.

Larger, E., Carel, J. C., & Boitard, C., 2005. Role of Beta -Cells in Type 1 Diabetes Pathogenesis. *Diabetes*, 54(1), S87–S96.

Lebovitz, HE., 2001, Effect of the postprandial state on non-traditional risk factors, *American Journal of Cardiology*, 88(6A), pp. 20H-25H. Lewin, B., 2004. Gene Expression. *Gene Expression*, 3(1), pp.64–75

Lin, L., DeMartino, G.N. & Greene, W.C., 1998. Cotranslational Biogenesis of NF- κ B p50 by the 26S Proteasome. *Cell*, 92(6), pp.819–828.

Ma, R.C. & Chan, J.C., 2013. Type 2 diabetes in East Asians: similarities and differences with populations in Europe and the United States. *Ann N Y Acad Sci*, 1281, pp.64–91.

- Marumo, T., Schini-Kerth, V.B. & Busse, R., 1999. Vascular endothelial growth factor activates nuclear factor-kappaB and induces monocyte chemoattractant protein-1 in bovine retinal endothelial cells. *Diabetes*, 48(16), pp.1131–1137.
- Nareika, A., Im, Y.-B., Game, B. A., Slate, E. H., Sanders, J. J., London, S. D., Huang, Y., 2008. High glucose enhances lipopolysaccharide-stimulated CD14 expression in U937 mononuclear cells by increasing nuclear factor kappaB and AP-1 activities. *The Journal of Endocrinology*, 196(1), 45–55.
- National center for biotechnology information (NCBI)., 2012. [online] U.S. National Library of Medicine. Available from: <http://www.ncbi.nlm.nih.gov/snp/?term=NFKB1> [Accessed February 2013].
- Nehme, A & Edelman, J., 2008, Dexamethasone inhibits high glucose -, TNF, and IL-1-induced secretion of inflammatory and angiogenic mediators from retinal microvascular pericytes, *Investigative Ophthalmology & Visual Science*, vol. 49 no. 5, pp. 2030-2038.
- New-England-Biolabs-Inc., 2010. Restriction Enzyme Troubleshooting Guide, NEB., pp.1–2.
- Nishikori, M., 2005, Classical and alternative NF-kB activation pathways and their roles in lymphoid malignancies, *Journal of Clinical & Experimental Haematopathology*, vol. 45 no. 1, pp. 15-24.
- Paneni, F., Beckman, J., Creager, M., & Cosentino, F., 2013. Diabetes and vascular disease: pathophysiology, clinical consequences, and medical therapy: part I. *European heart journal*, 34(31), pp.2436–43.
- Patel, S & Santani, D., 2009, Role of NF-kB in the pathogenesis of diabetes and its associated complications, *Pharmacological Reports*, vol. 61, pp. 595-603.
- Primer quest., 2013. [online] Integrated DNA Technologies. Available from: <http://eu.idtdna.com/PrimerQuest/Home/Index> [Accessed October 2013].
- Rohilla, A, Kumar, R, Rohilla, S & Kushnoor, A., 2012, Diabetic retinopathy: Origin and complications, *European Journal of Experimental Biology*, vol. 2 no. 1, pp. 88-94.
- Romzova, M., Hohenadel, D., Kolostova, K., Pinterova, D., Fojtikova, M., Ruzickova, S., Cerna, M., 2006. NFKB and Its Inhibitor IKB in relation to type 2 diabetes and Its Microvascular and Atherosclerotic Complications. *Human Immunology*, 67(9), 706–13.
- Roy, H., 2006. Vascular Endothelial Growth Factors (VEGFs) - Role in Perivascular Therapeutic Angiogenesis and Diabetic Macrovascular Disease. Department of Biotechnology and Molecular Medicine, University of Kuopio, pp. 1-81.

Sandhu, M. S., Weedon, M. N., Fawcett, K. A., Wasson, J., Debenham, L., Daly, A., Walker, M., 2009. Common variants in WFS1 confer risk of type 2 diabetes. *Europe PMC Funders Group*, 39(8), pp.951–953.

Sandip, P.A.D., Santani, 2009. Role of NF-KB in the pathogenesis of diabetes and its associated complications. *Pharmacological Reports*, 61(1734-1140), pp. 595-603.

Sankar, G. Michael J. M, & Elizabeth B. K., 1998. NF-κB AND REL PROTEINS: Evolutionarily Conserved Mediators of Immune Responses. *Immunology*, 16: 225-26, p.10.1146.

Saxena, S., 2012, *Diabetic retinopathy*, 1st edn, Jaypee Brothers Medical Publishers, New Delhi.

Schröder, S., Palinski, W. & Schmid-Schönbein, G.W., 1991. Activated monocytes and granulocytes, capillary nonperfusion, and neovascularization in diabetic retinopathy. *The American journal of pathology*, 139(1), pp.81–100.

Shanmugam, N., M. A. Reddy, M. Guha, and R. Natarajan., 2003. High Glucose-Induced Expression of Proinflammatory Cytokine and Chemokine Genes in Monocytic Cells. *Diabetes*, 52(May), pp. 1256–1264.

Semenza, G.L., 2001. HIF-1 and mechanisms of hypoxia sensing. *Current Opinion in Cell Biology*, 13(2), pp.167–171.

Serono, M., 2011. *Hormones and Me Diabetes Insipidus Hormones and Me. Living science, transforming lives.* (A. P. E. Group, Ed.), Australia: Merck Serono Australia Pty Ltd.

Sivaprasad, S, Gupta, B, Crosby-Nwaobi, R & Evans, J., 2012. Prevalence of diabetic retinopathy in various ethnic groups: A worldwide perspective, *Survey of Ophthalmology*, 57(4), pp. 347-370.

Song, M.K., Roufogalis, B.D. & Huang, T.H.W., 2012. Modulation of diabetic retinopathy pathophysiology by natural medicines through PPAR-γ-related pharmacology. *British journal of pharmacology*, 165(1), pp.4–19.

Song, S., Chen, D., Lu, J., Liao, J., Luo, Y., Yang, Z., Wang, J., 2011. NFκB1 and NFκBIA polymorphisms are associated with increased risk for sporadic colorectal cancer in a southern Chinese population. *PloS one*, 6(6), e21726, pp. 1-10.

Stratton, I. M., Adler, a I., Neil, H. a, Matthews, D. R., Manley, S. E., Cull, C. a, Holman, R. R., 2000. Association of glycaemia with macrovascular and microvascular complications of type 2 diabetes (UKPDS 35): prospective observational study. *BMJ (Clinical research ed.)*, 321(7258), pp.405–412.

- Tadhg, Colm., 2006. Bioinformatic detection and analysis of functionally important genetic variation, *Molecular and Cellular Therapeutics*, Royal College of Surgeons in Ireland.
- Tarr, J. M., Kaul, K., Chopra, M., Kohner, E. M., & Chibber, R., 2013. Pathophysiology of diabetic retinopathy. *ISRN ophthalmology*, 2013 (146), p.13.
- Thermo Fisher, S., 2015. RNA Sample Collection, Protection, and Isolation Support—Troubleshooting. Available at: <https://www.thermofisher.com/uk/en/home/technical-resources/technical-reference-library/nucleic-acid-purification-analysis-support-center/rna-sample-collection-protection-isolation-support/rna-sample-collection-protection-isolation-support-troubleshooting.html> [Accessed November 28, 2015].
- Vincze, T., Posfai, J. & Roberts, R.J, 2014. Nebcutter v2.0. [online] New England Biolabs. Available from: <http://tools.neb.com/NEBcutter2/> [Accessed October 2013].
- Williamson, R.T., 2009. Causes of diabetes. 1909. *The Practitioner*, 253(1718), p.37.
- Xiao, H., Gu, Z., Wang, G., & Zhao, T., 2013. The possible mechanisms underlying the impairment of hif-1 α pathway signaling in hyperglycemia and the beneficial effects of certain therapies. *International Journal of Medical Sciences*, 10(10), pp.1412–1421.
- Zhang, W, Liu, H, Al-Shabrawey, M, Caldwell, RW, & Caldwell, RB., 2011. Inflammation and diabetic retinal microvascular complications, *Journal of Cardiovascular Disease Research*, 2(2), pp. 96-103.